Multimodal Sensor-Fusion for Context-Aware Semi-Autonomous Control of a Multi Degree-of-Freedom Upper Limb Prosthesis

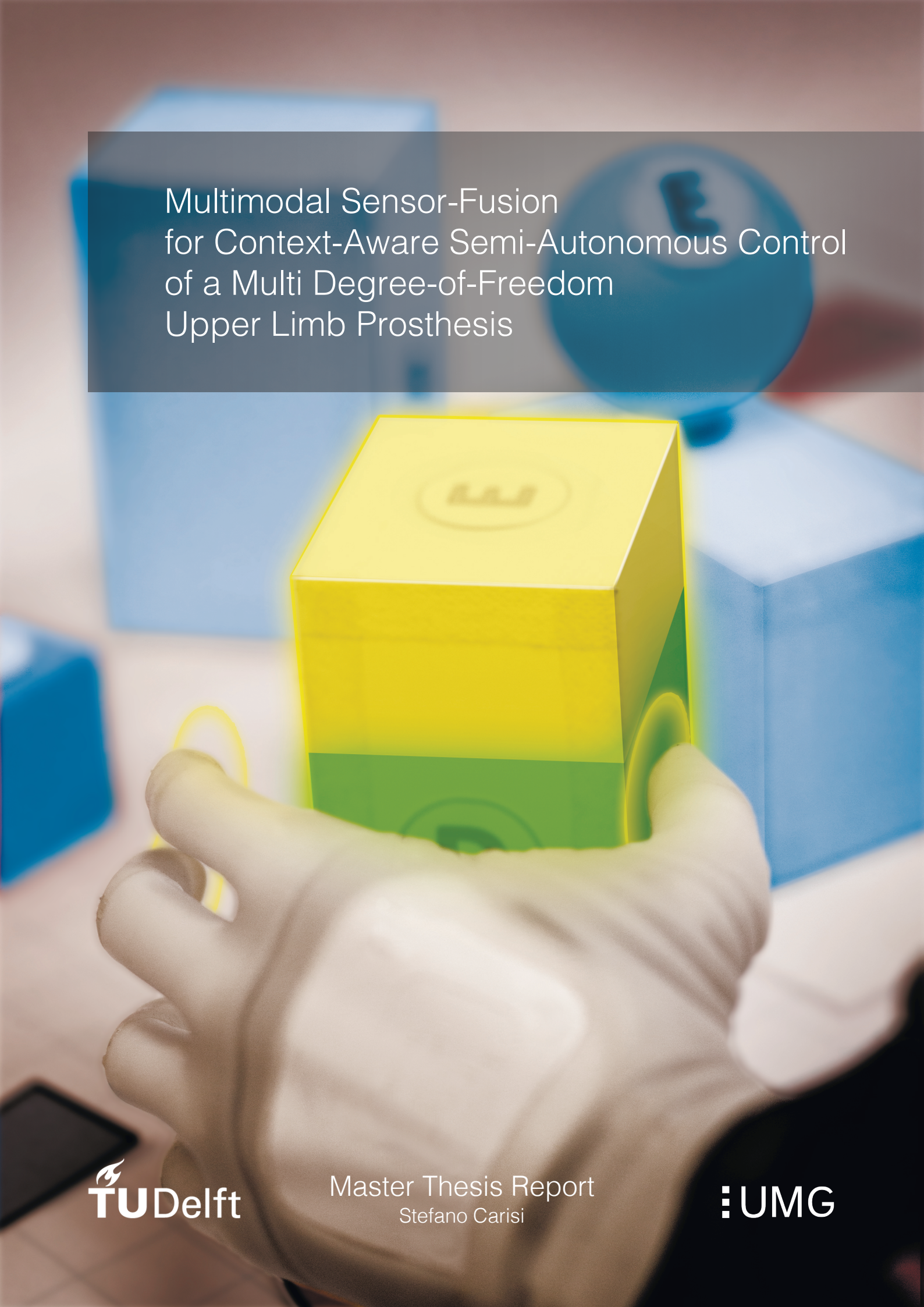

TU Delft

Master Thesis Report

Stefano Carisi

UMG

Page intentionally left blank.

Multimodal Sensor-Fusion for Context-Aware Semi-Autonomous Control of a Multi Degree-of-Freedom Upper Limb Prosthesis

(Master Thesis)

By

Stefano Carisi

in partial fulfilment of the requirements for the degree of

Master of Science
in Mechanical Engineering

at the Delft University of Technology.
to be defended publicly on Wednesday February 28, 2018 at 2:00 PM.

Student Number:	4434544	
Thesis Committee:	Dr.ir. D.H. Plettenburg,	TU Delft, Supervisor
	Dr.ir Marko Markovic,	UMG, Supervisor
	Prof.dr. Frans C.T. van der Helm,	TU Delft, Chair
	Prof.dr.ir. David Abbink,	TU Delft
	Dr.ir. Gerwin Smit,	TU Delft

TU Delft

UMG

Page intentionally left blank.

Nomenclature

ACM	-	Automatic Control Mode
ACU	-	Automatic Control Unit
AR	-	Augmented Reality
CASAC	-	Context-Aware Semi-Autonomous Control
DOF	-	Degree-of-freedom
(s)EMG	-	(surface)Electromyography
HMI(s)	-	Human-Machine Interface(s)
IMU	-	Inertial Measurement Unit
LCCP	-	Locally Convex Connected Patches
LDA	-	Linear Discriminant Analysis
MCM	-	Manual Control Mode
MCU	-	Manual Control Unit
MVC	-	Maximal Voluntary Contraction
RGB-D	-	Colour and Depth
RANSAC	-	Random Sample Consensus
SLAM	-	Simultaneous Localization and Mapping

Introduction

Hands are a highly dexterous tool which plays an essential role in humans' interaction with the world. Therefore, the sudden loss or congenital absence of hands can have a dramatic impact on a person's ability to perform work-related, social and daily living activities. One study has estimated that more than 541,000 upper limb amputees live in the United States alone [1].

The adoption of morphological and functional substitutions for the missing limb can alleviate the profound negative impact that amputation has on a person's life. Limb transplants are a way to achieve such substitution. However, between 1999 [2] and 2014 [3], only 70 successful cases of upper limb transplant have been reported due to the difficulties in finding the right donors and the necessary heavy immunosuppressive treatments. Prostheses adoption is a solution far more accepted in replacing the missing limb after an amputation. Prostheses have developed from simple cosmetic replacements into actuated systems: passive mechanic body-powered devices at first and mechatronic battery-powered active devices later on [4]. Battery-powered devices have been developed with the aim of reducing some drawbacks of the body-powered ones. The main drawbacks in body-powered prosthesis are the need for wearing a harness, the necessity for the user to generate high forces while operating the device, and their low morphological similarity to sound hands. Thus, a great variety of battery-powered devices is available nowadays. This include relatively simple single or multi degree-of-freedom (DOF) systems, like the Ottobock's Sensor Hand Speed [5] and Michelangelo Hand [6], and more complex mechatronic systems offering individual finger control and grasping capabilities close to the human hands [7], [8], like the Touch Bionics's i-Limb and the DARPA's prosthetic arm [9], [10].

Despite being the result of the long prostheses evolution and adopting cutting edge technological solutions, the battery-powered devices still have very high rejection ratios (23% of the amputees on average) or are used passively (27% of wearers) [11]. A closer look at the needs of upper limb prostheses users reveals possible reasons for such trends. Cordella et al. [12] reported two rudimentary categories of needs among upper limb prosthesis users: (1) those that are related to the morphological or physical properties of the prostheses (e.g., weight, comfort, durability) and (2) those that are related to the dexterity of the prostheses. In this study, I focus on dexterity, since this would address the majority of the suggestions for future prostheses developments listed by Cordella et al. [12], ultimately leading to increased myoelectric prostheses acceptance. Multiple factors can help improving the dexterity of the prostheses, such as providing sensory feedback, enabling precise and simultaneous control of several degrees of freedom, preventing object slippage, and precisely controlling applied forces on handled objects [12].

The aforementioned factors regarding prostheses' dexterity can all be addressed by improving the design of Human-Machine Interfaces (HMIs), through which users communicate with their prostheses. Almost twenty years ago [13], it was already recognized that simple, intuitive, and reliable interfaces for prosthesis control and feedback had to be developed. Nevertheless, modern interfaces are still far from being simple, intuitive and reliable. Therefore, the issue is still highly relevant [14]. Improving the HMIs designs is vital to improving prosthesis dexterity, and thus the dexterity-related factors listed above. According to Jiang et al. [15], HMIs for prosthesis control developed far slower than the robotic technologies they are interfaced with, becoming therefore inadequate for such systems [13], [16]. A multiplicity of HMIs have been developed over the last decades for efferent [17]–[19] and afferent [20]–[22] pathways in order to be employed in prosthetic devices control scenarios. Efferent interfaces are designed to decode high-level information (e.g., eat an apple) from users' neural activities (e.g.,

using electroencephalography or electrocorticography) and transmit commands to the prosthetic device. However, they are highly impractical for prosthesis control applications due to their complex instrumentation and low data transfer rates [17]. Therefore, interfaces that decode low-level signals, like muscle activations (e.g., electromyography (EMG) and mechanomyography), are often preferred for prosthesis control. Specifically, the myoelectric control interface is the state-of-the-art implementation in commercially available prostheses [15]. This type of interface decodes activations of forearm muscles into control commands proportional to the contraction intensity (i.e., proportional control). The user often needs to generate all the necessary input signals to operate the device because no form of automation [23] is implemented in most of the myoelectric control schemes. Myoelectric prostheses often do not include afferent interfaces either [12], [24], which are at the base of automation. Afferent interfaces are responsible for gathering information through sensors and transmitting them to the user or the computing unit. Afferent interfaces disregard, together with poorly designed efferent interfaces, makes the control of modern myoelectric prostheses tedious, unintuitive, and unnatural [25].

The importance of both efferent and afferent pathways can be seen in complex motor tasks. An ideal example is reaching and grasping. In this motor task, afferent pathways provide visual, tactile, and proprioceptive information to initially estimate, and later adjust, the motor commands sent through the efferent pathways for correctly shaping and orientating the hand [26]. Most importantly, for the majority of the time, the user is only actively concerned with the high-level control decisions (e.g., move a cup from a shelf to a table) while the low-level ones (e.g., hand aperture, grip force regulation) are handled subconsciously. During reaching and grasping, subconscious motor control requires multimodal afferent input to be processed by the human brain (vision, muscle spindles, Golgi tendon organs, joint receptors and skin receptors [27]). The state-of-the-art efferent interfaces in prosthetics, relying on myoelectric signals only, do not take advantage of multiple sensory inputs modalities, therefore making subconscious control impossible. As a result, the users have to consciously plan and directly perform all the necessary aspects of the task.

The ability of the prosthesis to independently and automatically perform a restricted set of actions, while simultaneously providing the user with direct control, is possibly the closest artificial counterpart to the natural human control. This is called semi-autonomous control. Research on semi-autonomous control with the aim of enhancing user experience has been performed for decades. Initial research focused on automatically selecting grasp type based on hand-to-object contact point [28]–[30]. Later on, more advanced systems were developed and commercialized for automatic reduction of users' compensatory movements during reaching [31] or object slippage avoidance [5], [32], [33]. In the last two decades, the increased interest in multimodal sensor-fusion approaches[1], which gather multimodal sensory inputs and interpret them using ad-hoc algorithms [34], facilitated new developments in semi-autonomous systems. New systems could automatically perform specific complex tasks after being triggered by the user [35], [36], or even by inferring users' behaviours [27], [37]–[41]. In particular, Markovic et al. [27] developed and tested a semi-autonomous system for prosthesis preshape during grasp tasks. The system mimics human motor control by replacing the biological sensors involved in hand preshaping with mechatronic ones: human eyes, proprioceptors, and somatosensory receptors are replaced by cameras, gyroscopes, motor encoders, and force sensors. The system developed by

[1] I could retrieve approximately 100 papers regarding sensor-fusion systems to analyze this trend. The number of published papers increased steadily, between 125% and 200%, every five years since the first few papers found in 1989. Nevertheless, the calculated rate of growth does not consider the fact that historic documents might not be available in digital format and therefore I could have missed them by performing only an electronic search. Yet, being the trend strongly visible between the years 2002 and 2017, when most of the research has been presumably published online, I assume that these findings can be trusted.

Markovic et al. outperformed the state-of-the-art of commercially available myoelectric controllers [27].

In this study, the system developed by Markovic et al. [27] has been upgraded by adding retroreflective markers and a prosthetic wrist with both flexion/extension and pronation/supination active degrees of freedom. The retroreflective markers made the system aware of the position of the prosthesis in space, while the two degrees-of-freedom wrist allowed for precise preshaping during grasping tasks. The sensor-fusion algorithm at the core of the system has also been improved, permitting system's usability in cluttered scenarios and accurate estimation of users' grasp intentions.

The aim of this study was to develop a system that complements the academic myoelectric state-of-the-art prosthetic control methodologies during the interaction with objects (e.g., grasping, manipulation) with the goal of increasing the overall robustness and performances of the prosthetic device. The second aim was to define guidelines, based on the acquired experimental data, for a larger-scale experiment to be performed in the immediate future. Two tests were designed to evaluate the performances, robustness and usability of the developed system in cluttered scenarios. These tests required the user to interact with multiple objects by reaching, grasping, reorienting, and repositioning them. The time to complete each trial and the number of drops have been recorded. These data have been used to evaluate system performance and robustness, respectively. The developed system has been compared with the myoelectric state-of-the-art control by performing the tests with both the control schemes. The novel system supplements the myoelectric control scheme by adding automation to it, therefore it is expected to perform better.

Paper

Multimodal Sensor-Fusion for Context-Aware Semi-Autonomous Control of a Multi Degree-of-Freedom Upper Limb Prosthesis

Stefano Carisi

Abstract

Objective. Dexterous control of myoelectric upper limb prosthesis is still limited by the capabilities of the modern human-machine interfaces. The first goal of the current work was to develop a system that supplements the academic myoelectric state-of-the-art interface during the interaction with objects (e.g., grasping, manipulation) with the goal of increasing the overall performances and robustness of the prosthetic device. Additionally, the current study aims to define guidelines for a larger-scale experiment to be performed in the immediate future. *Approach.* I developed algorithms, which provide context- and user-awareness to the system by fusing multimodal sensory input data, and a control scheme that employs such context-awareness to estimate the user's grasp intentions to automatically preshape the prosthesis for grasping in real time. The control scheme was compared against the major academic state-of-the-art myoelectric control scheme (i.e., pattern recognition) in two able-bodied subjects. The experimental tests consisted of grasping, reorienting, and relocating sets of common objects using a multi-degree-of-freedom prosthesis with two grip types and two degrees-of-freedom actuated wrist. *Main Results.* The proposed semi-autonomous system was able to function in realistic and time-varying cluttered environments. The obtained results illustrate better and more consistent performances (i.e., lower task completion time and standard deviation) of the developed control scheme with respect to the state-of-the-art counterpart. Improvements in control robustness during object manipulation (i.e., lower number of object drops) have also been obtained. The current study helped in defining guidelines for the future larger-scale experiment: more than one experimental session, data logging and subjective measurements recording. *Significance.* The proposed system improves multiple aspects involved in the control of myoelectric multi-degree-of-freedom upper limb prostheses. The guidelines defined in this work, are essential for evaluating, during the future larger-scale study, the impact of the proposed system on users' experience (e.g., workload and ease of use).

1. Introduction

Hands are a highly dexterous tool which plays an essential role in humans' interaction with the world. Therefore, the sudden loss or congenital absence of hands can have a dramatic impact on a person's ability to perform work-related, social and daily living activities. Myoelectric prostheses are the result of a long evolutionary process to provide morphological and functional replacement to missing limbs. They are mechanically very advanced and mimic closely sound hands' degrees of freedom [7] allowing, among others, individual finger movements and up to 24 different grip patterns over the 33 that are possible with a sound hand [8]. Nevertheless, myoelectric prostheses have still very high rejection ratios (23% of the amputees, on average) or are passively used (27% of wearers) [11]. Cordella et al. [12] reported that one of the primary complaints of upper limb amputees was the low dexterity of their prostheses. Thus, dexterity is critical for improving the user acceptance of myoelectric prostheses. Multiple factors can help improve the dexterity of a prosthesis, such as providing sensory feedback, enabling precise and simultaneous control of several degrees of freedom, preventing object slippage, and precisely controlling applied forces on handled objects [12].

The aforementioned factors regarding prostheses' dexterity can be addressed by improving the design of Human-Machine Interfaces (HMIs), through which the users communicate with their prostheses. According to Jiang et al. [15], HMIs for prosthesis control developed far slower than the robotic technologies they are interfaced with, becoming, therefore, inadequate [13], [16]. A multiplicity of HMIs have been developed over the last decades for efferent [17]–[19] and afferent [20]–[22] pathways in order to be employed in prosthetic control. Interfaces can decode high-level information (e.g., eat an apple) or low-level ones (e.g., muscle activation). Interfaces for high-level decoding have been tested several times in the attempt to provide valid substitutes for myoelectric interfaces. However, they are highly impractical for prosthesis control due to their complex instrumentation and low data transfer rates [17]. Therefore, low-level interfaces, like the myoelectric ones, are still the state-of-the-art implementation in commercially available prostheses [15]. Nevertheless, these interfaces include no form of automation and the users often need to generate all the necessary input signals in unintuitive,

and unnatural manners [25]. Newer approaches in myoelectric control have been developed to provide more natural and intuitive control. One of these is pattern recognition, often implemented using the Discriminant Analysis (LDA) method, which analyses the patterns generated by the contraction of multiple forearm muscles and associates independent prosthesis motions to each of them. This approach showed promising initial results and quickly became the state of the art in the academia, but found only recently a limited translation into commercial applications (COAPT [42]) mainly due to its lack of robustness [43]. Myoelectric interfaces based on pattern recognition, though, rely only on low-level information and didn't address the limitations related to the absence of automation. Systems employing myoelectric control often underestimate afferent interfaces and feedback [12], [24], which are at the base of automation. Afferent interfaces are responsible for gathering information through sensors and transmitting them to the user or the computing unit. Afferent interfaces disregard, together with poorly designed efferent interfaces, makes the control of modern myoelectric prostheses tedious, unintuitive, and unnatural [25].

The myoelectric HMIs in prosthetics have been significantly improved by a technique called multimodal sensor-fusion. For this reason, multimodal sensor-fusion approaches are gaining popularity in research. They rely on afferent interfaces to gather multimodal input information, which is then fused (i.e., combined) together using ad-hoc algorithms that estimate high-level user intent. Importantly, multimodal sensor-fusion techniques distinguish themselves from the conventional interfaces, which can combine data obtained from multiple sensors but all belonging to the same modality (unimodal sensor-fusion). Relying on multiple sensor modalities, multimodal sensor-fusion systems can interpret user's behaviour and surroundings so as to implement some degree of automation. This generally increases ease of use, robustness, or performance compared to what is achievable by each interface involved in the system when considered independently [44], [45]. Obtaining context-awareness is an approach widely spread in multimodal sensor-fusion for wheelchair drive ([46], [47], [48], [49]), but it is recently gaining popularity in upper limb prostheses control. The myoelectric interfaces have been supplemented by systems for automatic reduction of users' compensatory movements during reaching using IMU data [50], object slippage avoidance by interpreting force sensor data [5], [32], [33], or automatic grasp estimation thanks to computer vision [27], [37]. In particular, Markovic et al. [27] developed and tested a semi-autonomous system for prosthesis preshape during grasp tasks. The system mimics human motor control by replacing the biological sensors involved in hand preshaping with mechatronic ones: human eyes, proprioceptors, and somatosensory receptors are replaced by cameras, gyroscopes, motor encoders, and force sensors. The system developed by Markovic et al. outperformed the state-of-the-art of commercially available myoelectric controllers [27].

In this study, the system developed by Markovic et al. [27] has been upgraded by adding retroreflective markers and a prosthetic wrist with both flexion/extension and pronation/supination active degrees of freedom. The retroreflective markers made the system aware of the position of the prosthesis in space, while the two degrees-of-freedom wrist allowed for precise preshaping during grasping tasks. The sensor-fusion algorithm at the core of the system has also been improved, permitting system's usability in cluttered scenarios and accurate estimation of users' grasp intentions. Overall, the system developed in this study exploits a multiplicity of proprioceptive and exteroceptive sensing units to closely mimic the natural human control techniques. It gathers information which is naturally used by humans performing grasping tasks: a depth camera is used for visual assessment of the workspace; a gyroscope, retroreflective markers, and motor encoders provide knowledge on prosthesis pose, position, and orientation in space; a force sensor is employed for object interactions estimation. Myoelectric signals are also recorded and used as direct user control inputs. All the collected inputs are processed by the ad-hoc sensor-fusion algorithm, which is responsible for estimating high-level user intentions (e.g., targeted object, desired grasp type) and performing low-level tasks accordingly (e.g., hand aperture and wrist orientation adjustments). The control loop is closed by providing the user with Augmented Reality (AR) information about the state of the system and the decisions made by the algorithm. As a result, the system and user collaborate towards the common goal of object interaction: the algorithm supports the user in low-level controls while the user focuses on the high-level decisions (e.g., where to position the hand, what to do with the object) and just seldom fine-tunes the system's decisions.

The aim of this study was to develop a Context-Aware Semi-Autonomous Control (CASAC) system that complemented the academic myoelectric state-of-the-art prosthetic control methodologies during the interaction with objects (e.g., grasping, manipulation) with the goal of increasing the overall robustness and performances of the prosthetic device. The second aim was to define guidelines, based on the acquired experimental data, for a larger-scale experiment to be performed in the immediate future. Two tests were designed to evaluate the performances, robustness and usability of CASAC in cluttered scenarios. These tests required the user to interact with multiple objects by reaching, grasping, reorienting, and repositioning them on a table. The time to complete each trial and the number of drops have been recorded. These data have been used to evaluate system performance and robustness, respectively. CASAC has been compared with LDA by performing the tests with both the control schemes. The developed system supplements LDA by adding automation to it, therefore it is expected to perform better than LDA alone.

2. Materials and methods

2.1 Overall control system operation

The conceptual scheme of the implemented semi-autonomous control system is depicted in Figure 1. The system can operate in two control modes: Automatic Control Mode (ACM) Figure 1(A) selected by default, and Manual Control Mode (MCM) Figure 1(B). The ACM relies on the system's context-awareness to infer user intentions and accordingly adjust the corresponding DOFs of the prosthesis. Specifically, the ACM performs two actions simultaneously: it gathers information on the environment and updates its model, and automatically preshapes the prosthesis. The MCM, instead, allows the user to manually control the prosthesis by generating appropriate myoelectric control signals that are decoded in corresponding myoelectric control commands for the prosthesis. The user can switch from ACM to MCM by generating any valid myoelectric control command (IF block (1) in Figure 1). All the ACM functions (i.e., *Scene Model/Lock* and *Prosthesis Preshape/Freeze*) are automatically paused when the user switches to the MCM. Once

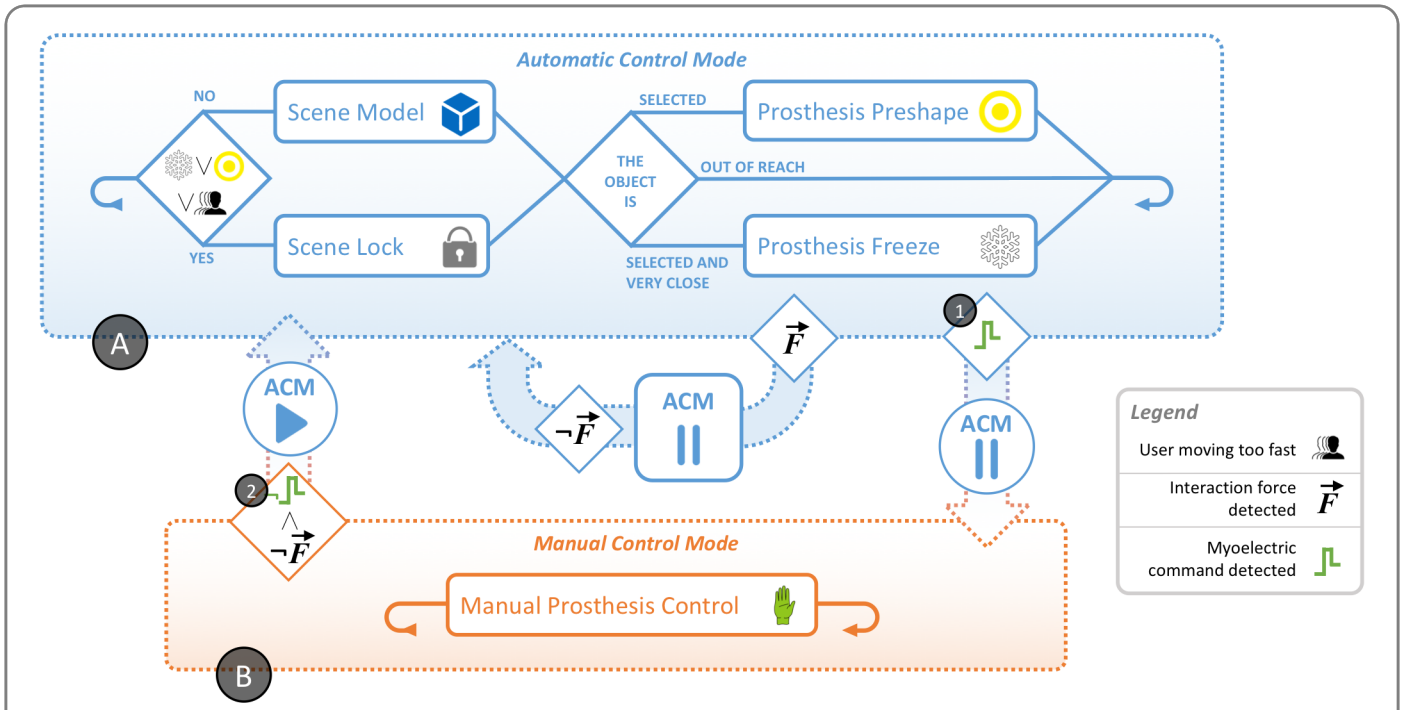

Figure 1 | Conceptual Scheme of the Semi-Autonomous control system. The system operates either in Automatic Control Mode (ACM), the default one, or in Manual Control Mode (MCM). The user can take manual control over the prosthesis by generating valid myoelectric control commands, which will switch the control of the prosthesis to the MCM and simultaneously pause the ACM. When the system is in ACM (subfigure A), information is continuously captured from user's surroundings and decisions are taken in real time regarding the preshaping of the prosthesis. The ACM performs two distinct functions simultaneously: updates the model of the environment (*Scene Model/Scene Lock*) and preshapes the prosthesis (*Prosthesis Preshape/Prosthesis Freeze*).

in MCM, the system will automatically return to ACM if the user is neither sending myoelectric commands nor manipulating any object (IF block (2) in Figure 1). To recognize if the user is manipulating an object, the system relies on the force sensor integrated on the prosthesis thumb: detection of an interaction force after a manual myoelectric command to close the prosthesis implies that an object has been grasped and that the manipulation phase has begun. When the manipulation phase is over, the system switches back to the ACM, resuming its functions. The ACM can also be paused to prevent objects tilting or breaking. This is identified by the system when the prosthesis is automatically preshaping and a force is detected.

The overall system operates as a state machine, where two groups of states are simultaneously active: the first group concerns the prosthesis preshaping (includes *Manual Prosthesis Control, Prosthesis Preshape*, and *Prosthesis Freeze* states), whilst the second one refers to the scene surrounding the user (*Scene Model* and *Scene Lock* states). These states follow a hierarchical structure, where the *Manual Prosthesis Control* has the biggest influence, being responsible for pausing the Automatic Control Mode and therefore deactivating all the other states. *Prosthesis Preshape* and *Prosthesis Freeze* are second in order of importance since they have direct influence over the scene-related states (*Scene Model* and *Scene Lock*).

The prosthesis preshaping states are regulated according to the following set of rules:

1. In case myoelectric control commands are detected, the prosthesis is fully manually controlled (*Manual Prosthesis Control*)
2. When the prosthesis is in the proximity of an object, this object is tagged as selected and the prosthesis is automatically preshaped for grabbing it optimally (*Prosthesis Preshape*).
3. If an object is selected and the prosthesis is very close to it, the system assumes that the user will grasp the selected object. Therefore, in order to provide the user with a stable condition for grasping, the prosthesis' DOFs are not adjusted. This also prevents involuntary contacts with the object due to unexpected automatic movements (*Prosthesis Freeze*).

Importantly, in case the prosthesis would be too far from any object, and no myoelectric control command is sent, the prosthesis would receive no instructions from the system.

The states regarding the scene surrounding the user function as follows:

1. In *Scene Model* state, a new update of the scene is computed every frame. When the scene is updated, the objects' models are recomputed, meaning that their shapes, positions, sizes, and orientations get updated.
2. The *Scene Lock* state is triggered when any of these two criteria is verified: the user is selecting an object (prosthesis adjusting or frozen) or moving too fast in the scene. The first condition is necessary to avoid modelling incomplete objects when the prosthesis is in their proximity, partially occluding them from camera's sight. The second condition has been included to cope with the delay intrinsically present in modelling the scene. Practically, if the user is moving fast, the camera is also moving fast and the new frame will be captured from a strongly different point of view compared to the previous one. This would make the

link between the two scenes very hard to be found. Not updating the scene when the user is moving fast does not interfere with the objective of this study. In the tests performed in this study the user is involved in grasping only stationary objects, an activity generally performed while moving at low speed and steadily observing the object.

2.2 System Prototype

The system prototype comprises the following components: (1) eight 13E200 dry EMG electrodes with integrated amplifiers (Otto Bock Healthcare GmbH, Vienna, AT), (2) Michelangelo left-hand prosthesis with active wrist rotator and flexor module (Otto Bock Healthcare GmbH, Vienna, AT) mounted on a custom-made support (i.e., socket), (3) an MTx Inertial Measurement Unit (IMU) (XSens Technologies B.V., Enschede, NL), (4) Meta Glasses Development Kit 1 (Meta Company, San Mateo, CA), (5) Creative SR300 camera (Creative Technology Ltd, SG), (6) three retroreflective markers (19-mm diameter), and (7) a processing unit (i.e., a standard desktop PC with 16GB RAM and 8-core i7@4.0 GHz CPU). Figure 2 illustrates the relevant components.

The *myoelectric interface* comprises an array of eight dry active electrodes evenly distributed over subjects' forearm muscles, on the ipsilateral side of the prosthesis. The electrodes with adjustable gains acquired the EMG data and directly provided the smoothed signals (linear envelopes) which did not require low-pass filtering. The linear envelopes were sampled at 100 Hz and transferred to the host PC via the Bluetooth connection.

The *Michelangelo hand prosthesis* provides simultaneous opening and closing of all fingers with two grip types (palmar[2] and lateral[3]), as well as actuated wrist pronation/supination and flexion/extension [6]. The prosthesis is mounted on a custom-made ergonomic socket which is connected to the left forearm of able-bodied subjects, positioning the prosthesis below the hand and in a more distal position. The four position encoders (thumb, fingers, wrist rotator and wrist flexor) measure fingers aperture and prosthesis orientation relative to the socket. A single force transducer positioned at the base of the thumb measures the grasping force. A bidirectional communication protocol, running over a Bluetooth interface at 100 Hz, allows the prosthesis for sensory data transmission and control commands reception.

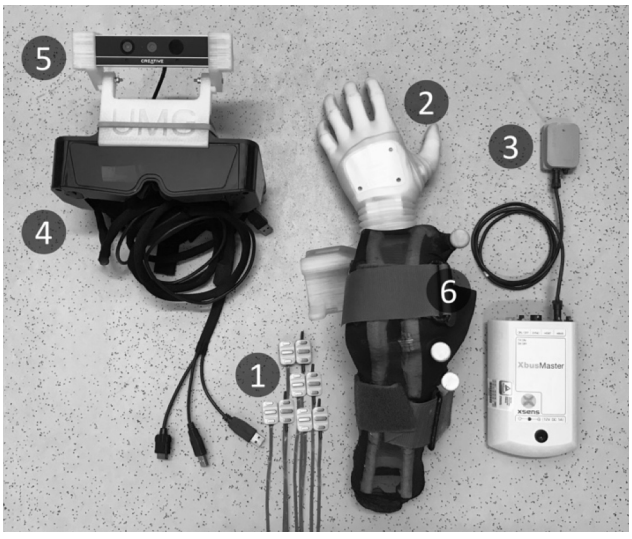

Figure 2 | System components. The system comprises (1) eight dry surface EMG electrodes, (2) a prosthesis with two grip types, active wrist and flexor, (3) an inertial measurement unit, (4) augmented reality glasses, (5) a color and depth camera, (6) three retroreflective markers and a standard PC (not illustrated in the figure).

The *IMU* is attached to the custom-made socket through a 3D printed connector. The IMU measures the absolute orientation of the prosthetic hand with respect to the laboratory coordinate system (i.e., yaw, roll and pitch angles) and streams data to the host PC at a sampling rate of 30 Hz through a battery-powered acquisition and wireless transmission unit (XBus, XSens Technologies B.V., Enschede, NL).

The *AR Meta Glasses*, connected to the computer through an HDMI wired connection, superimpose digital holographic images to the real world, allowing the user to receive visual feedback directly on the scene she/he is interacting with. The holographic images are generated by projecting, with a refresh rate of 30 Hz, 960×540 pixels screens on two semi-transparent glasses located in front of user's eyes. The Meta Glasses also embed an inertial sensor and a 320×240 pixels depth camera, which, due to their low resolutions, have been replaced by the Creative SR300 camera sensors in the current system.

A *Creative SR300 camera* is mounted on the glasses worn by the subject by using a 3D printed support. This ensures that the camera is facing the same scene that the user is looking at. It simultaneously acquires and streams, at 30 Hz through a USB port, both colour and depth (RGB-D) images [45] at a resolution of 1920×1080 pixels and 640×480 pixels, respectively. The depth data are acquired using the embedded infrared camera, while the RGB-D data is used for ego-motion estimation.

The three *retroreflective markers* are placed on the custom-made forearm splint in positions that prevent occlusion while performing the tasks. The relative position of the markers is captured at 30 Hz by the infrared sensor of the SR300.

The *host PC* (1) receives data from sensors of the prosthesis, the myoelectric interface, the inertial unit, and the camera; (2) processes them to obtain context-awareness and make decisions regarding the prosthesis control; (3) sends control commands to the prosthesis and (4) visualize feedback on the augmented reality glasses. Likewise, the host PC also provides a user interface for experimental protocol execution (e.g., starting, stopping), system setup and monitoring. The algorithms are implemented using C++ for scene generation, Unity 3D (Unity Technologies, San Francisco, US) for scene management, prosthesis preshaping and AR feedback, MATLAB 2017a and Simulink (MathWorks, Natick, US-MA) for myoelectric inputs decoding (CLS Toolbox [51]).

2.3 Control flow and algorithm implementation

The novel context-aware sensor-fusion control scheme integrates an Automatic and a Manual Control Unit (ACU and MCU), illustrated in Figure 3(A) and Figure 3(B) respectively. The outputs of these two units are mixed in the Decision Mixing Unit (Figure 3(C)), which is in charge of simultaneously and

[2] the tip of the thumb opposes against the tip of other digits

[3] the pad of the thumb against the lateral side of the index

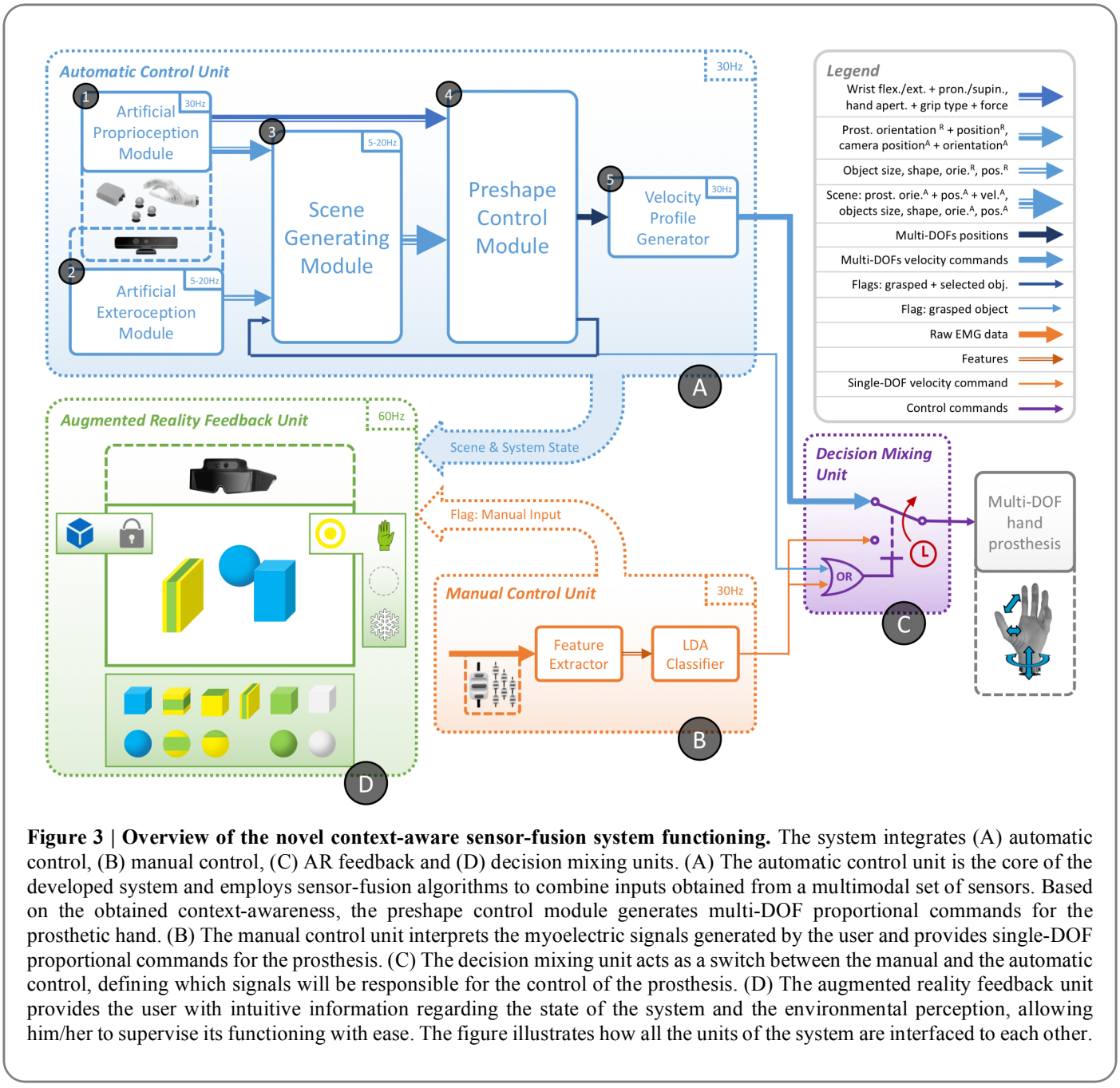

Figure 3 | Overview of the novel context-aware sensor-fusion system functioning. The system integrates (A) automatic control, (B) manual control, (C) AR feedback and (D) decision mixing units. (A) The automatic control unit is the core of the developed system and employs sensor-fusion algorithms to combine inputs obtained from a multimodal set of sensors. Based on the obtained context-awareness, the preshape control module generates multi-DOF proportional commands for the prosthetic hand. (B) The manual control unit interprets the myoelectric signals generated by the user and provides single-DOF proportional commands for the prosthesis. (C) The decision mixing unit acts as a switch between the manual and the automatic control, defining which signals will be responsible for the control of the prosthesis. (D) The augmented reality feedback unit provides the user with intuitive information regarding the state of the system and the environmental perception, allowing him/her to supervise its functioning with ease. The figure illustrates how all the units of the system are interfaced to each other.

proportionally controlling the multiple degrees of freedom of the prosthesis. Lastly, the Augmented Reality Feedback Unit (Figure 3(D)) provides AR visual feedback to the user based on the information received from the ACU and the MCU.

A. Automatic Control Unit

The ACU (Figure 3(A)) comprises two sensory input modules (Artificial Proprioception Module and Artificial Exteroception Module), two data elaboration modules (Scene Generating Module and Preshape Control Module) and one output converter (Velocity Profile Generator). The aim of the ACU is to estimate user's intentions based on the information acquired about the environment and the user itself, so as to automatically provide the Decision Mixing Unit with simultaneous and proportional control inputs for the prosthesis.

The *Artificial Proprioception Module* (Figure 3(A.1)) implements acquisition and pre-processing of the signals recorded from information sources about the user's body parts position and orientation in space (i.e., hand tracking and ego-motion), including prosthesis pose (i.e., DOFs configuration) and interaction force. The module provides two outputs: (1) pose of the prosthesis relative to the splint and interaction force; (2) position and orientation of the user[4] and his/her left forearm in space. The module collects digital signals assessing the current state of the prosthesis and converts them into user-readable information based on the internal prosthesis model (i.e., wrist

[4] When reading about user's position and orientation, the reader should be aware of the fact that these terms refers to the position and orientation of the camera that the user is wearing on his/her head. This choice on the wording has been made to simplify the explanation, since the camera is connected as a rigid body with user's head and oriented along his/her vision direction.

flexion/extension, hand pronation/supination in degrees, hand aperture in centimetres, lateral/palmar grip type, and interaction force in Newtons). These data correspond to the first output of the module. The software implemented in the camera automatically sets an absolute reference frame on the first frame captured during initialization and provides then ego-motion information (i.e., camera orientation and position) based on it. The camera also captures the position of the threes retroreflective markers located on the prosthesis. A model is fitted on the markers and its orientation is used, during the calibration phase, to transform the IMU orientation (provided in the laboratory coordinate system) into the camera reference frame. Once calibrated, the IMU data will be used to determine the orientation of the prosthesis with respect to the user. Tracking the prosthesis position by integrating the IMU acceleration would result in high noise. Therefore, the retroreflective markers are used to track the prosthesis position in space. A Kalman filter is used to generate the best estimate for the real prosthesis position during the current frame, functioning even when up to two markers would temporally be out of sight. The errors for prosthesis positions and orientation in space are estimated to be <1 cm and <5º. The implemented algorithm is illustrated in detail in Appendix Figure 1.

The *Artificial Exteroception Module* (Figure 3(A.2)) acquires depth images of the environment through the RGB-D camera and uses computer-vision algorithms to model the objects present in the scene (i.e., it estimates their shape, size, position and orientation relative to the camera reference system). The Locally Convex Connected Patches (LCCP, [52]) and Random Sample Consensus (RANSAC, [53]) algorithms are used on a pre-processed point cloud (i.e., filtered) in order to cluster its points and model the objects, respectively. The objects are fitted as basic geometrical shapes (spheres, boxes) and require no a priori knowledge about their properties (e.g., colour features, size). The detailed steps of the algorithm, together with the used filtering parameters are described in (Appendix Figure 2).

The *Scene Generating Module* handles the updates of the scene surrounding the user using Simultaneous Localization and Mapping (SLAM) [54] techniques. The inputs of this module contain all the proprio- and exteroceptive information collected by the system (except for prosthesis' pose and interaction force), and an indication (i.e., flag) from the Preshape Control Module about selected or grasped objects. The output of the module is the model of the scene surrounding the user (in absolute coordinates) with the addition of prosthesis velocity. The module is subdivided into two sub-systems schematized in Appendix Figure 3. The first subsystem transforms the input coordinates, expressed in the camera-relative reference frame, into absolute coordinates. It also calculates the velocity of the user and of his/her prosthesis and averages it over the last five samples (approximately 0.15 s). The second subsystem is responsible for updating the scene, deciding whether to lock it or not. When the scene updating function is invoked, it collects all the new object models from Artificial Exteroception Module and tries to match them individually with the old ones, using the Hungarian algorithm [55]. If a new model is matched, it joins the set of latest elements for that specific object. Up to ten latest elements are stored for each object set. If an incoming model is not matched with any previous object model, a new set is generated for it. The best element of each set is then selected using the Mahalanobis distance criteria [56]. These elements represent the new update for the objects visible in the scene and will be shown to the user through the AR glasses. Additionally, the implemented SLAM algorithms retain out-of-sight objects in the scene even if no new models are available for them. For details about the algorithm implementation, the reader can refer to Appendix Figure 3. The scene updating function is invoked only when user's velocity is below the predefined threshold and the prosthesis is neither selecting nor grasping an object, as previously explained in *Section 2.1*. Selection and grasping information is available to this module as feedbacks from the Preshape Control Module. As soon as an object is grasped, it is also removed from the scene, since the user is manipulating it. When the user releases the object, it will be remodelled in the new position.

The *Preshape Control Module* represents the core of the Automatic Control Unit, where an advanced sensor-fusion algorithm combines intelligently all the information available to the system (proprioception and exteroception) to obtain context-awareness and make appropriate decisions on the prosthesis preshape. The output of this module is the set of DOF coordinates variations necessary for orienting the prosthesis toward the target object. The algorithm is composed by two sub-systems: (1) the first one determines the object to select (i.e., target) and (2) the second one computes the optimal prosthesis orientation (rotation, flexion) and preshape (grasp type, aperture) for grasping it.

Subsystem 1 - Each object in the scene is assigned a semi-circular selection area, which surrounds the object as illustrated in Figure 4 (light blue shapes). When the prosthesis enters the selection area of an object, a positive selection coefficient for that object is computed. This coefficient is inversely proportional to the distance of the prosthesis to that object. The object with the highest selection coefficient is marked as selected. Once an object is selected, its selection area expands (yellow shape in Figure 4) and helps to stabilize the selection decisions, especially in cluttered environments. Another important role in object selection is played by the non-circular shape of the selection area: it allows for quick deselections of an object when the prosthesis moves at its right side, avoiding unnatural pronation movements. Lastly, the system avoids

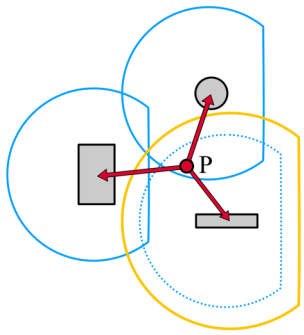

Figure 4 | Object selection area representation. Each object is surrounded by a selection area (light blue shape). The distance (red arrow) between the prosthesis (P) and each object determines the corresponding selection coefficient (inversely proportional to the prosthesis-to-object distance if the prosthesis is inside the selection area, null otherwise). The object with the highest coefficient is marked as selected and its selection area is extended (yellow shape). This stabilizes the selection.

selecting objects located along the path to the target object by enabling object selection only when the prosthesis velocity is below a predefined threshold. Appendix Figure 4(Subsystem 1) provides details on the selection algorithm.

Subsystem 2 - In order to preshape the hand, the system has to perform three decisions: grip type, wrist orientation and hand aperture. First of all, lateral grip type is selected if the prosthesis forward direction is oriented toward the small side of a flat object, or the object itself is small. In any other case, palmar grip type is selected. Then, the relative position between the prosthesis and the object is used to infer user's intention of grasping the object from the top or from the side/front. Rotation and flexion of the wrist are regulated such that the fingers involved in the grasp (i.e., index, middle finger, and thumb) are directed toward the centre of the object. Depending on the condition (lateral grip, top or side/front palmar grip), small adjustments of the DOFs are performed to facilitate the grasp and prevent interference with the surface on which the objects are lying (i.e., the table). Lastly, the hand aperture has to be computed. As a first step, the plane which is both passing through the object centre and normal to the hand-to-object vector is used to generate a cross-section area. The size of the cross-section along the closing direction of the fingers determines the required minimum aperture for grasp. Various tests have been performed to evaluate the error involved in computing the hand aperture. Uncertainties of the prosthesis and of the object orientation play a dominant role over the aperture size error. Errors up to 1.5 cm in aperture size estimations have been recorded. Therefore, the desired hand aperture is selected 2.5 cm bigger than the calculated minimum, allowing error compensation and facilitating object grasping. Appendix Figure 4(Subsystem 2) provides details on the prosthesis preshape algorithm.

The *Velocity Profile Generator* implements the position control of the prosthesis by regulating its velocity in real-time. The output of this block is a set of velocities that can be directly processed by the multi-DOF hand prosthesis.

B. Manual Control Unit

The MCU (Figure 3(B)) acquires raw EMG signals from the array of eight EMG electrodes located on the ipsilateral side of the subject, extracts features and classifies them into proportional single-DOF velocity commands for the prosthesis. Root mean square features are extracted and Linear Discriminant Analysis (LDA) is used for their classification. Seven classes have been implemented to control the DOFs of the prosthesis: close lateral, close palmar, open, flex, extend, pronate and supinate. When the EMG signals are matched with the *open* class, the prosthesis opens maintaining the current grip type (palmar/lateral). Additionally, the threshold for activating this class is automatically raised when the user is manipulating an object and moving it in the workspace at high speed. This functionality has been implemented based on the assumption that the user intends to relocate objects safely in the workspace, without dropping or throwing them (i.e., releasing an object while moving at high speed). The system is expected to be more robust if the prosthetic hand does not open during object manipulation. The context-awareness of the system makes this functionality trivial to implement.

C. Decision Mixing Unit

The Decision Mixing Unit (Figure 3(C)) is ultimately responsible for deciding which of the two control inputs (autonomous, or manual) will be connected to the prosthesis. It operates as a switch reset by a timer. The default state of the switch lets the Automatic Control Unit handle the movements of the prosthesis. When myoelectric control commands are detected, or an object is grasped, the switch changes its state and the control commands generated by the Manual Control Unit are transmitted to the prosthesis. If no manual commands are supplied for longer than 1.5 seconds and no object is grasped, the timer included in the switch automatically gives the control back to the Automatic Control Unit.

D. Augmented Reality Feedback Unit

The Augmented Reality Feedback Unit (Figure 3(D)) is responsible for providing the user with visual feedback regarding the system states and scene perception through augmented reality glasses. The module gathers the scene details and the system state from the ACU, in addition to a flag indicating manual control commands from the MCU. The outputs of the module are displayed on the semi-transparent AR glasses. Icons are presented to the user on the top corners of the field of view. On the top-left, the state of the scene (updating the models or not) is displayed. On the top-right, the current state of preshaping control (automatic preshape, manual preshape, no preshape because of no object selected, no preshape because of prosthesis too close to the selected object) is displayed. The rest of the display is used to visualize the virtual objects present in the scene. All objects' holograms are blue by default. When an object gets selected, its colour changes to yellow with a green stripe which intuitively indicates to the user the decision made by the system. A horizontal green stripe indicates front/side palmar grip, a vertical green stripe indicates lateral grip, the green top face of the object indicates top palmar grip. This colour pattern is presented in Figure 3(D). Getting too close to the object will freeze the prosthesis, which is indicated to the user by colouring the selected object in white. Lastly, when manual commands are sent, the object will turn green, indicating that the user acquired full control over the prosthesis.

The system workflow consists of multiple steps. The camera models the environment to obtain context-awareness (Scene Modelling state). The modelling state icon is shown to the user on the upper left corner of the AR glasses. Once the scene is modelled, blue 3D models representing the real objects are superimposed and rendered on the AR glasses, Figure 5.

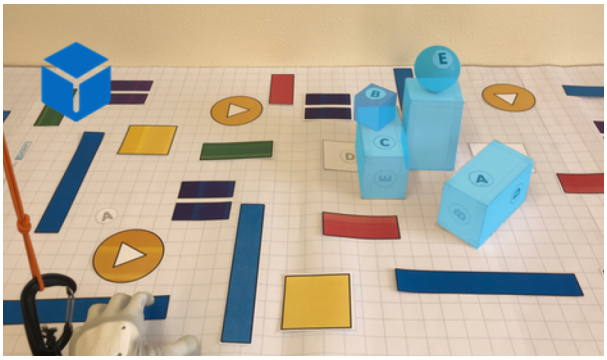

Figure 5 | Workflow Step 1. The objects in the scene are modeled and blue holograms are presented to the user. The top-left icon indicates the system is in Scene Modeling state.

The scene continues to get updated until the user, approaching an object for grasp, places the prosthesis inside the selection area of an object. When this happens, the scene is locked (Scene Locked state, icon visualized on the glasses) and the object is selected. The selection icon is visualized on the right side of the glasses, indicating the Prosthesis Preshape state. The projection of the selected object in the glasses assumes a yellow-green texture. The texture with a green horizontal stripe indicates that the system inferred user's intention to grasp the object from the front/side in palmar mode. This estimate was made based on the relative position of prosthesis and object. The prosthesis is automatically preshaped for grasping the object, Figure 6.

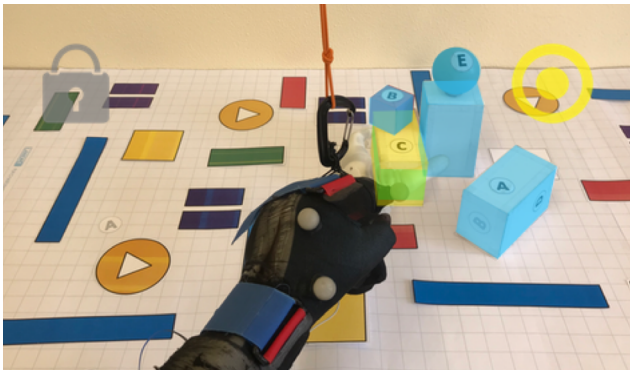

Figure 6 | Workflow Step 2. The system infers user intention to grasp object C from the front/side. The object assumes a yellow-green texture, the prosthesis is preshaped, and the Scene Locked state and Prosthesis Preshape state icons are displayed.

The user changes his mind and decides to grasp another object in the scene. When two objects are next to each other and their selection areas overlap, whichever object with a higher selection-coefficient is selected by the system. The colours of object C and A in Figure 7 get updated. The hand preshape is adapted for the new grasp (palmar grip, approaching the object from above).

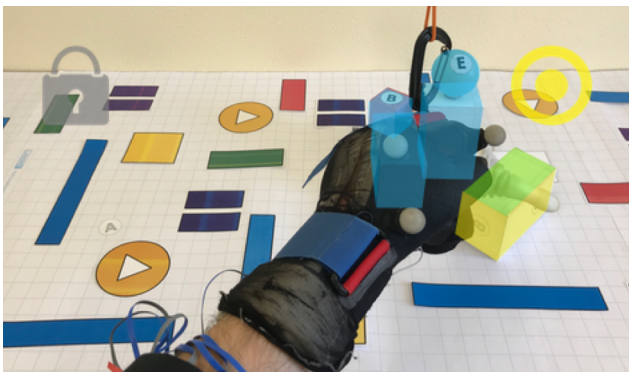

Figure 7 | Workflow Step 3. Object C gets deselected and object A assumes the yellow-green texture indicating palmar grip for grasping the object from above.

The user decides to grasp the newly selected object from the left side. While he/she is moving the prosthesis to the side of the object, its preshape gets continuously adjusted based on the relative prosthesis-to-object position. When the intention of a side-grasp is detected, major adjustments to the DOF are performed so as to orient the prosthesis for this type of grasp, Figure 8.

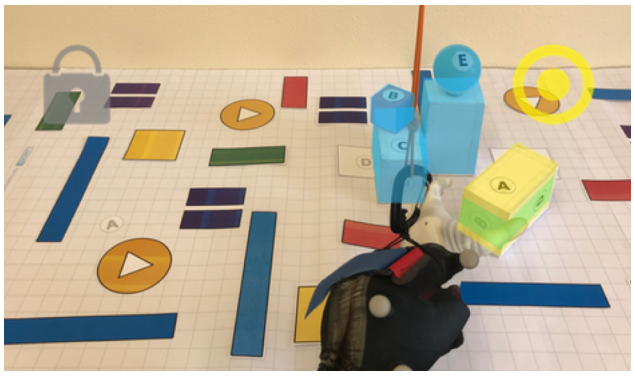

Figure 8 | Workflow Step 4. The user moves the prosthesis and side grasp intention is detected. The object texture is updated and the prosthesis reshaped accordingly.

While the user gets closer to the object, the prosthesis preshape speed is proportionally decreased based on the distance from the object, mimicking human natural approach [57]. When the prosthesis is almost touching the object, this is recognized by the system and the prosthesis gets frozen to prevent unintentional interactions with the object. The object is shown in white colour to indicate the new state of the system (Prosthesis Freeze) and the *freeze* icon is shown on the glasses instead of the *selection* icon, Figure 9.

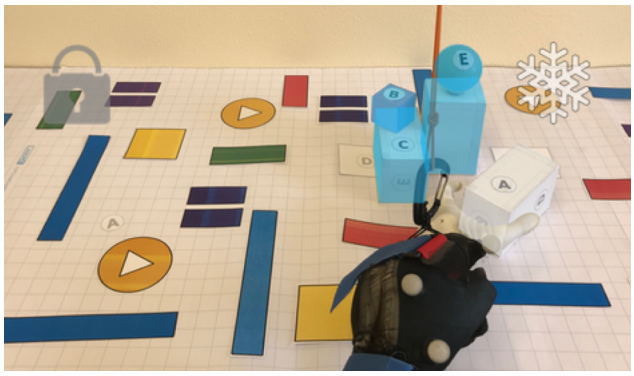

Figure 9 | Workflow Step 5. The user is almost touching the object. The prosthesis is frozen. The Prosthesis Frozen state icon is visualized and the object turns white.

The user decides to grasp from a slightly different angle and therefore contracts is left forearm muscles to generate the myoelectric pattern for prosthetic wrist flexion (i.e., flexing his/her hand). The object becomes green while the DOFs of the prosthesis are manually adjusted and the Manual Prosthesis

Control icon is visualized on the top-right corner of the glasses, Figure 10.

Figure 10 | Workflow Step 6. The user takes full control of the system by generating muscle activity. The hologram of the target object becomes green and the Manual Prosthesis Control icon is visualized.

Within 1.5 seconds from the wrist angle adjustment, the user triggers the LDA class for hand closing. The hand closes and the object is grasped. The hologram of the object is destroyed and the manipulation in manual control mode begins, Figure 11.

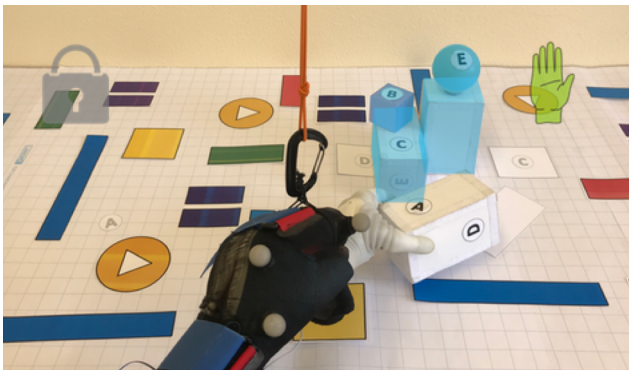

Figure 11 | Workflow Step 7. The user grasps an object. The corresponding hologram is destroyed.

Once the object is released, the system returns in Step 1 and resumes the modelling the objects, including the one that has just been released, Figure 12.

It should be noted that it is not necessary to complete all the steps to fulfil the task. Depending on the user, or on the task to be performed, this sequence might vary (e.g., Step 5 will be skipped if the user issues manual commands before the prosthesis is frozen).

2.4 Experimental protocol

Subjects. Two male right-handed healthy subjects, aged 24 and 29, volunteered for this study. All subjects gave written consent to participate in the experiment and had previous experience in LDA myoelectric control.

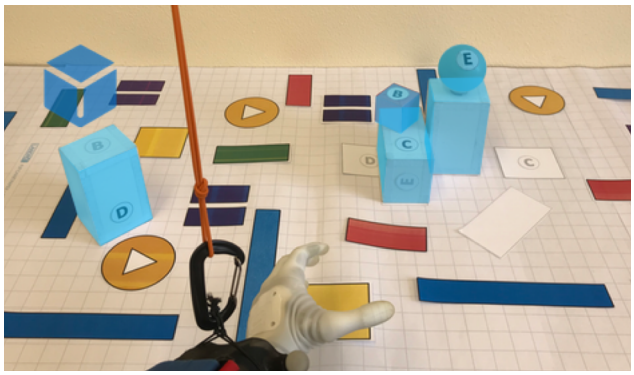

Figure 12 | Workflow Step 8. The system resumes from Step 1 and the newly repositioned object is modeled in the new position.

Setup. The subjects wore the system and stood in front of a table (L 200 × W 105 × H 70 cm). Several objects were placed on the table and labelled with letters. The participants were required to move each object to its destination position. The destination positions were indicated with labels matching the objects' ones, and printed shapes, indicating the required final orientations. The destination positions were located both on the table and on slots in the wall facing the user. The initial positions of the objects, the participant, and the prosthesis were the same within testing scenarios. The subjects were allowed to move along the table while performing the experiments as much as they pleased. The subjects were instructed not to perform visibly exaggerated compensatory movements to complete the tasks. Being allowed to move along the table, they were able to compensate for the missing adduction/abduction DOF in the prosthetic wrist. The left hand was fitted in a custom-made ergonomic socket which was strapped firmly using Velcro straps to the subjects' forearm. The prosthesis was located below the subjects' hand and in a more distal position. The splint immobilized the hand, resulting in isometric muscle contractions during EMG signals generation. The more distal position of the prosthesis with respect to the real fit in amputees resulted in higher torques applied on users' arm joints (i.e., elbow, shoulder) during usage, increasing fatigue. To compensate for this effect, and creating a testing scenario closer to amputees' conditions, the prosthesis has been connected to an elastic element located above the table which generated a lifting force able to partially diminish the experienced weight. The array of eight dry EMG electrodes was placed on the ipsilateral side of the prosthesis, approximately five centimetres below the elbow joint, resembling the inside-socket mounting location for amputees. The subjects wore the AR glasses with the attached RGB-D camera and the IMU master acquisition unit was strapped around the waist and placed on the back. The setup is illustrated in Figure 13.

System Initialization and Calibration. The system is initialized as soon as the camera is turned on and the first frame is acquired. This frame is used by the system for ego-motion estimation and for reference during IMU calibration. Ego-motion estimation works best when the captured images present a high contrast. For this reason, the table presented a high contrast pattern (visible in Figure 13). Three components required calibration before the system could adequately be used:

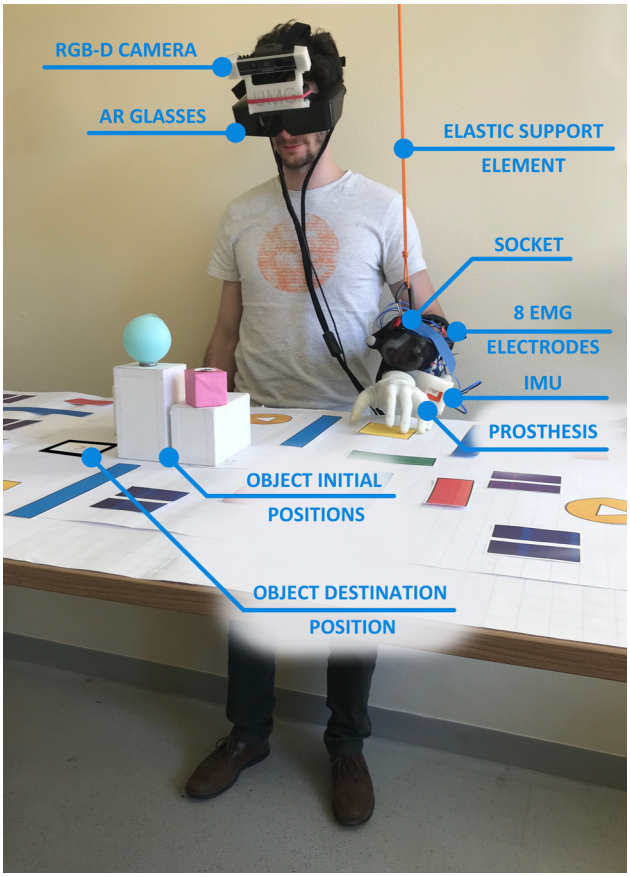

Figure 13 | Experimental setup overview. The figure illustrates the visible system components and setup elements. The initial positions for the user and the prosthesis at the beginning of a trial are as shown in the figure.

the AR glasses, the IMU and the myoelectric interface. The holographic projection in the glasses had to be calibrated once per subject to cope with both the biological diversities between users and the way they wore the glasses. Specifically, eyes position, position of (middle of) image plane, orientation of image plane, and (horizontal) field of view had to be calibrated. A calibration setup has been developed and used for this purpose, making sure that the generated holographic objects would ultimately superimpose precisely with the real objects. The AR glasses calibration setup, together with an example of both uncalibrated and calibrated holograms projection, is shown in Appendix Figure 5. The IMU orientation had to be calibrated before every trial: the user wore the splint with the prosthesis on his left arm and held it motionless on the table, looking at it. The orientation offset between the model of the three retroreflective markers located on the splint and the IMU was computed. This offset was used to set the relative orientation of the IMU with respect to the user. The myoelectric interface was calibrated before each test session in three different arm positions (shoulder 75° extended and 30° horizontally abducted, shoulder 75° extended and 30° horizontally adducted, shoulder 60° extended). To achieve adequate calibration, the subjects were first instructed on how to generate consistent and distinguishable muscle patterns. The myoelectric control was then calibrated in three steps: the isometric maximal voluntary contractions (MVC) for each LDA class were measured; the classes at three levels of contraction (35%, 50%, 70% of the MVC) were trained; the classes' gains and thresholds to adjust the reactivity of the prosthesis were fine-tuned. The prosthesis was driven at the maximum velocity allowed for each DOF when the muscle activity reached approximately 70% of the MVC.

Procedure. The performances of the developed context-aware semi-autonomous control (CASAC) scheme were evaluated by comparison with the myoelectric state-of-the-art LDA control. Each control scheme has been assessed by performing two different tests with it. For each test, two different scenarios have been developed by rearranging the objects on the table while maintaining their orientations. The usage of two different scenarios reduced the risk of obtaining results strongly correlated to the specific configuration used and allowed to estimate the capability of the CASAC system in modelling the different scenes. Figure 14 illustrates the two tests, the four scenarios and the objects in their destination positions.

During the experiment, the subjects had to interact (i.e., grasp, lift, reorient, transport and release) with a set of objects using once the CASAC and once the LDA control for each of the two tests:

Test 1: five objects (boxes of different sizes and a cylinder) were placed on the table far apart from each other and not overlapping, as illustrated in Figure 14 (1,2). In this test, the subjects interacted with each object only once. This test aimed at showing the performances of the CASAC system in situations where it was fundamental to constantly update the scene (i.e., remove the grasped objects) for the correct system functioning.

Test 2: five objects (boxes of different sizes and a sphere) were placed on the table close to and stack on each other, creating a cluttered scene. In this test, the subjects interacted with objects located both at the base of the stack and at the top of it. Additionally, the subjects had to interact with some objects more than once, bringing these objects to a temporary destination, perform other interactions, and later interact with them again. This test allowed made me estimate if the semi-autonomous system could cope with cluttered scenarios, where continuous real-time understanding of a quickly varying scene is necessary, in addition to the system's ability to correctly estimate subjects' desired selections in complex situations.

A training phase (approximately 30 minutes) preceded the experiment. During the training phase, the participants tried both the CASAS and the LDA control, in every scenario. The training phase allowed the subjects to understand the behaviours of the semi-autonomous system, as well as practising in selecting and proportionally controlling the prosthesis' DOF by generating appropriate muscle activations. While practising, the subjects also received explanations about the movements generated by each of the control schemes (CASAC, LDA). To ensure that the subjects understood the AR feedback, they received an explanation on what each feedback element meant. Furthermore, the subjects practised in using the manual control for overruling the CASAC decisions. After the training phase, the subjects felt confident in their ability of skilfully interacting with the systems during the testing session.

The participants rested for approximately 10 minutes after the training phase to reduce the effects of muscle fatigue before starting the experiment. In this experiment, the specific combination of a control scheme (i.e., CASAS and LDA) and a test type (i.e., Test 1, Test 2) will be addressed as "test condition". Therefore, a total of eight test conditions has been completed in a pseudo-randomized order. For each test

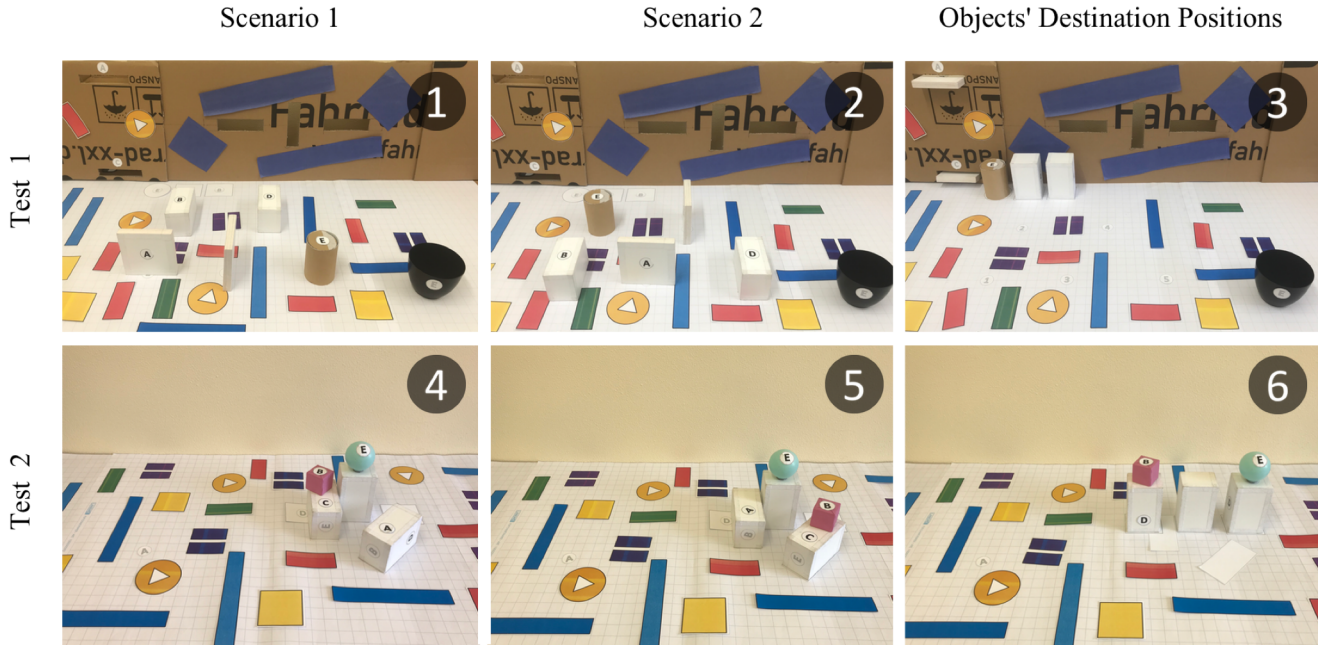

Figure 14 | Tests, scenarios, and objects in their destination positions. This figure illustrates the initial positions for the objects in the different test scenarios (1,2,4,5). In subfigure 3 and 6 are shown the positions of the objects at trial completion (i.e., their destination positions). The point of view of the images has been chosen to match closely the one of subjects standing in front of the table on the indicated starting position.

condition, seven trials have been performed. Within each trial, two minutes of rest were given to the participants. For each test condition, the first two trials have not been recorded and had the only purpose of getting the subject familiar, once more, with the scene and the system. Among the recorded five trials per test condition, only the last three were used for data analysis, in an attempt to mitigate the influence of learning. There was no time limit for performing the trial, but the subjects were instructed to perform it as fast as possible while at the same time avoiding excessive compensatory movements. No instructions were given regarding how to grasp or manipulate the objects. Only the specific order of interaction with the objects was defined. When using the CASAC, the prosthesis was preshaped in real-time depending on its relative position to the objects and the subjects could take direct control of the preshape at any moment by generating appropriate muscle patterns. The state of manual commands was kept active for 1.5 seconds after a contraction had been detected, therefore giving enough time to the subjects to generate another command if needed (e.g., adjust the wrist rotation and then close the hand). The experimenter observed the task execution and the trial was repeated in the following cases: (1) while using CASAC, the subject uninterruptedly provided manual commands, preventing the automatic unit from preshaping the prosthesis; (2) the user performed strong compensatory movements; (3) the subject dropped any of the objects while performing the trial; (4) any main hardware/software component stopped functioning, therefore compromising system operation. The trial was not considered over until all the objects had been relocated to the destination positions and oriented correctly. At the end of every trial, the user moved back to the starting position, placed the prosthesis on the predefined initial position on the table and looked at it for IMU calibration. The scene was reorganized by the experimenter, the virtual scene of the CASAC was destroyed (no previous knowledge about the scene configuration is passed to the next trial), and the prosthesis was reset to its neutral position.

2.5 Data Analysis

The primary outcome measure was the trial time (TT) in each test condition, assessing the efficacy in operating the prosthesis based on the particular control used. The TT was measured, from the start of the trial until its completion, using the timer implemented in the GUI developed to allow the experimenter to supervise the system functioning.

The secondary outcome measure was the number of times the subject had to repeat the trial because of object drops (OD). This measure assesses the robustness of the control system during preshaping and manipulation.

Due to the limited number of participants involved in this pilot study, no statistical trend could be inferred. Therefore, the author limited the data analysis to the calculation of means and standard deviations for the primary outcome measure for each participant. The number of retrials due to object drops is also analysed independently for each subject.

3. Results

In total, 112 trials (2 subjects × 1 session × 8 test conditions × 7 trials) have been performed and 48 of those have been analysed (2 subjects × 1 session × 8 test conditions × 3 trials).

Figure 15 shows the trial time (mean ± standard deviation measured in seconds) and the number of object drops for each subject and test condition during the experiment. Compared to

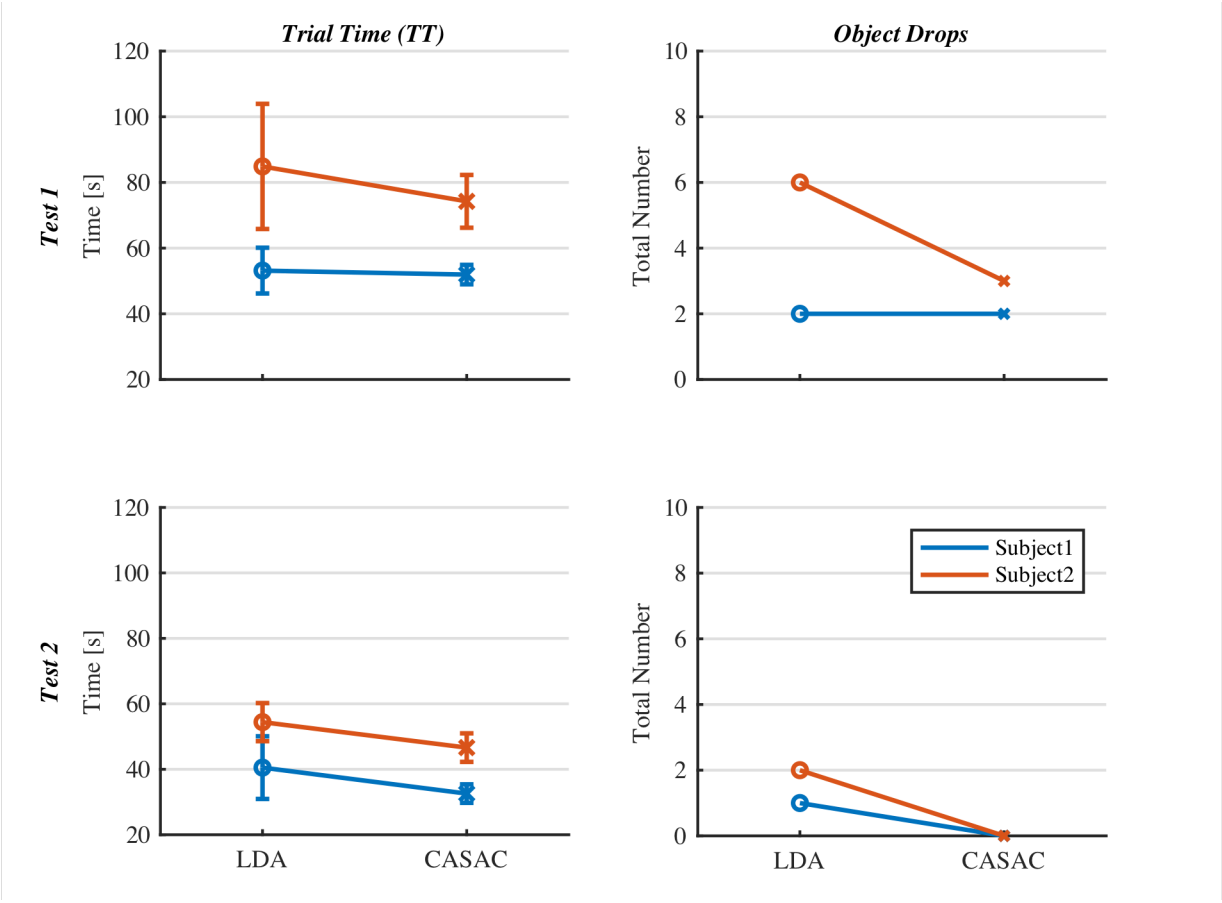

Figure 15 | Summary results for the two control schemes in each test type. The results ((mean ± standard deviation) for average time to grasp (TT) and total number of object drops) are presented for each subject, test and control scheme. Notations: CASAC — Context-Aware Semi-Autonomous Control; LDA — Linear Discriminant Analysis myoelectric control.

the LDA control scheme, both trial time means and standard deviations decreased for all the subjects when performing the tests using the novel CASAP control. In Test 1, the average TT of Subject1 were 53.2 ± 6.7 s and 51.9 ± 3.0 s for LDA and CASAS, respectively. Subject2, instead, completed Task 1 with an average TT of 84.9 ± 19.1 s and 74.2 ± 8.0 s for LDA and CASAS, respectively. In Test 2, the average TT decreased from 40.5 ± 9.6 s and 54.4 ± 5.8 s to 32,6 ± 2.8 s and 46.6 ± 4.4 s between LDA and CASAS control schemes, respectively. Therefore, the mean TT is on average 12.2% smaller in CASAS with respect to LDA, with lower improvements in Test 1 (2.3% and 12.5%) with respect to Test 2 (19.6% and 14.3%). The standard deviation of the trial times was higher in LDA (52.7% on average) with respect to CASAP. The total number of object drops varied widely among subjects. In test 1, Subject 1 had the same number of drops with both the control schemes. Subject 2 obtained, instead, a 50% reduction in object drops (from 6 to 3) when using the CASAC. In test two, both the subjects had no drops while using CASAC, while they had 1 and 2 with the LDA control scheme.

4. Discussion

Test 1 was designed to evaluate if the system is able to keep track of a quickly changing scene, constantly updating it and making decisions accordingly. Test 2 was designed to examine the system's ability to cope with cluttered scenarios and correctly estimate subjects' intentions. The findings of this study show a general improvement in subjects' performances when the context-aware semi-autonomous control (CASAC) scheme is supplementing the academic state-of-the-art myoelectric LDA control scheme. Even if no significant difference could be found among the results, the findings indicate a favourable trend for the system's ability to function in cluttered scenarios, keeping track of time-changing environments and of understanding subjects' grasping intentions in such situations. A future larger-scale study will allow evaluating any statistically significant difference exists between the two control schemes.

The standard deviations in the mean time to complete the trials, when supplemented by the CASAC scheme, decreased by approximately 50%, compared to the LDA myoelectric control. This suggests that CASAC had consistent behaviours or/and that it was more intuitive to use. These favourable trends should be confirmed by increasing the sample size in future studies. To evaluate the consistency of the CASAC, data logs should be collected and analysed to determine if the system took coherent decisions when similar conditions occurred (e.g., consistently orient the DOFs of the prosthesis when proximal to objects with same sizes and orientation). The intuitiveness of the CASAC could instead be investigated in future studies by combining the outcomes of questionnaires with the learning trends obtained by performing multiple experimental sessions (two or three).

The reduced number of object drops while using the CASAC scheme is a potential indicator of system robustness. I believe that the implemented functionalities to limit unwanted prosthesis behaviours could have reduced object drops. One of these functionalities is stopping the automatic prosthesis preshape when it inadvertently hits an object or gets very proximal to it. Another functionality is the automatic threshold increase for the LDA opening class while the prosthesis is moving fast in space. In future tests, analysis of the data log files could be a good approach to examine the system behaviours. For instance, finding opening class activations within the standard threshold and the raised one during objects relocation would indicate that the developed functionality avoided object drops.

The functionalities implemented in this system can be considered a good starting point for demonstrating the potential of sensor-fusion approaches applied to prosthetic control. The proposed system can quite easily be extended with the ability to cover experimental setups as wide as a room, or with the possibility to support the pattern recognition algorithms in various aspects (e.g., reduce arm position influence over classification accuracy [58], vary classes activation levels depending on probabilistic factors). Another interesting functionality to implement would be the automatic preshape of the prosthesis based on the sound hand movements, allowing for bimanual interactions with objects or to easily pass them from one hand to the other. To achieve such functionality, it would only be necessary to add an inertial sensor to the sound hand (e.g., smartwatch, bracelet with integrated IMU) and account for this component in the sensor-fusion algorithm. Another option is to act on the intelligence of the Decision Mixing Unit of the CASAC, therefore varying the shared-control paradigm and leading to new forms of human-machine interactions in prosthesis control. At the moment, the Decision Mixing Unit operates as a switch connected to a timer. A more sophisticated algorithm might, for instance, join and weight the contributions of the automatic and manual control inputs to the output depending on the context. Lastly, the presented sensor-fusion approach could be extended to similar fields of application, like rehabilitation robotics, by controlling exoskeletons instead of prostheses.

This study was limited by (1) the small number of participants, which did not allow to recognize possible statistically significant differences; (2) the presence of only one experimental session, which did not allow the author to draw conclusion regarding the learning curve of the subjects with the two control schemes; (3) the absence of data logging, which could play a relevant role in tracking the decisions of the system at every instant in time, gaining an understanding of how these decisions affected the overall performance of the system; (4) the absence of subjective measures, like an extended version of the NASA-TLX questionnaire [59] that includes questions regarding the general acceptance of the novel concept, which would give insights into the overall user experience.

5. Conclusion

The prototype described in the present study represents a substantial step ahead with respect to the earlier works of Markovic et al. [27], [40], [60]. It integrates many new functionalities which have previously been recommended for future developments [27]. Specifically, the system adopts sophisticated SLAM-based approaches and advanced tools for depth-image analysis to cope with cluttered and complex scenes, allowing for a continuous and reactive understanding of the user surroundings. Furthermore, the developed system almost entirely removed the experimental constraints present in the last study of Markovic et al. [27]. The only constraint left is due to the length of the camera cable, which limits the user distance from the host PC. This factor aside, the users can move as pleased in an unconstrained experimental environment and their interactions with the objects present in the setup are far more intuitive (object selection and automatic preshape triggering). These results were achieved by adding software and hardware components to the system to increase its user- and context-awareness. Specifically, the implemented ego-motion algorithms allowed to estimate user position in space, while the included retroreflective markers allowed for precise prosthesis tracking. The additional prosthetic wrist flexion/extension active degree-of-freedom might have also contributed to the overall capability of the subjects to interact with the multiplicity of grasping situations encountered in the proposed experimental setups. The semi-autonomous context-aware system developed in this study is able to simultaneously and proportionally control multiple degrees of freedom, a notable result that brings myoelectric control closer to mimicking human biological motions [57].

My findings indicate that the semi-autonomous context-aware system developed in this study is feasible for prosthesis control and is able to increase performances and robustness of the state of the art academic myoelectric control scheme (i.e., pattern recognition). It also lays the basis for the development of more complete studies to address unanswered questions. Specifically, future studies should include (1) more subjects to evaluate statistical differences between the proposed control scheme and the state of the art one; (2) data logging to objectively evaluate system's decision, and (3) subjective measures (e.g., NASA-TLX questionnaire [59]) to evaluate workload. Two or three experimental sessions are suggested for future studies, so as to gain data about the learning curve of the CASAC system with respect to the pattern recognition control. I also recommend to include amputees in the subjects' pool, as they are the intended users of this technology.

As a final remark on the performed study, I would like to underline that the employed ad-hoc tests have been specifically designed to evaluate the overall applicability of the novel system prototype in prosthesis control. While designing the tests, the focus has been put on performing a relevant set of tasks requiring multi-DOF adjustments. The usage of ad-hoc tests is not unusual in the scientific literature when evaluating *ready-to-use* systems [36], [61]. I am conscious of the efforts put by the scientific community into establishing standardized evaluation benchmarks [62]–[64] and believes that, when the system approaches clinical applicability (which includes components integration and miniaturization for usage in practical scenarios), standardized tests will have to be performed.

Appendix

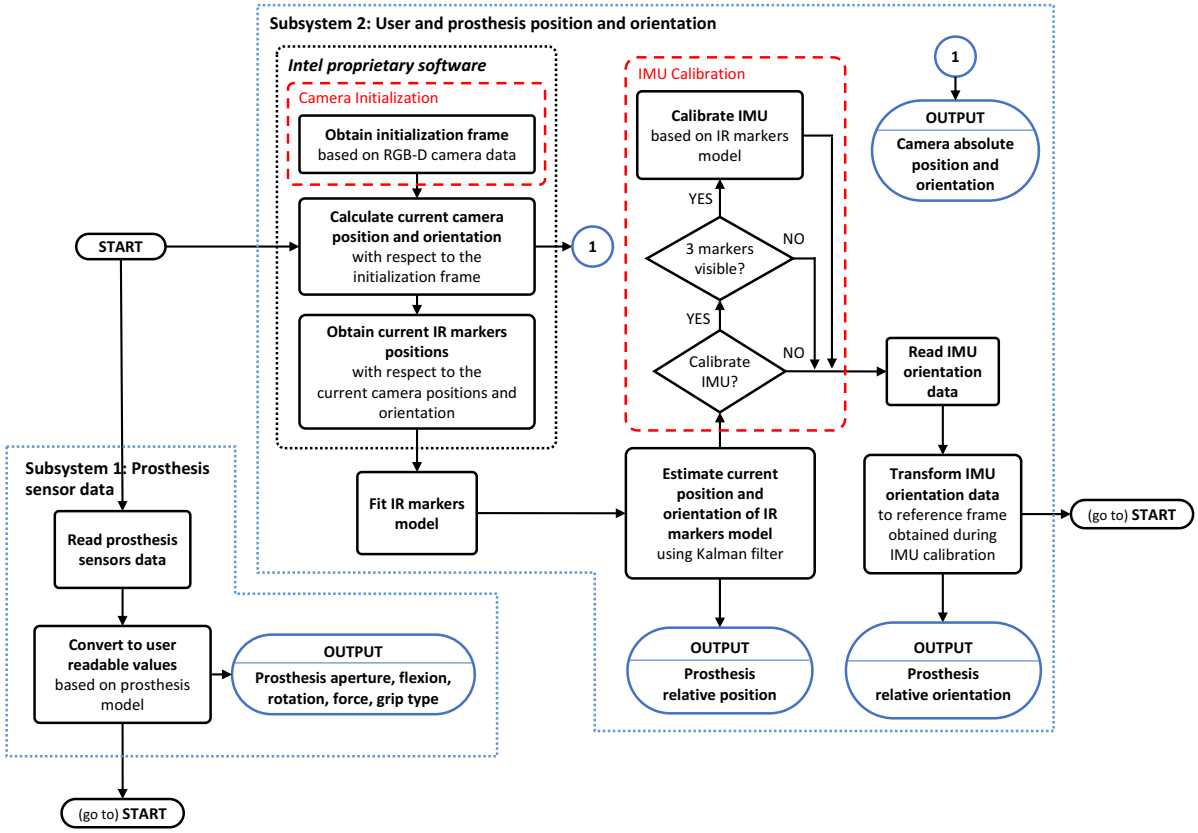

Appendix Figure 1 | Artificial Proprioception Module algorithm. The algorithm consists of two subsystems: the first one analyzes and converts the prosthesis sensor data; the second one estimates position and orientation of both user (i.e., camera located on his/her head) and prosthesis. The camera is automatically initialized when the system is started (camera initialization red block); the IMU calibration is instead performed before each trial (IMU Calibration red blocks).

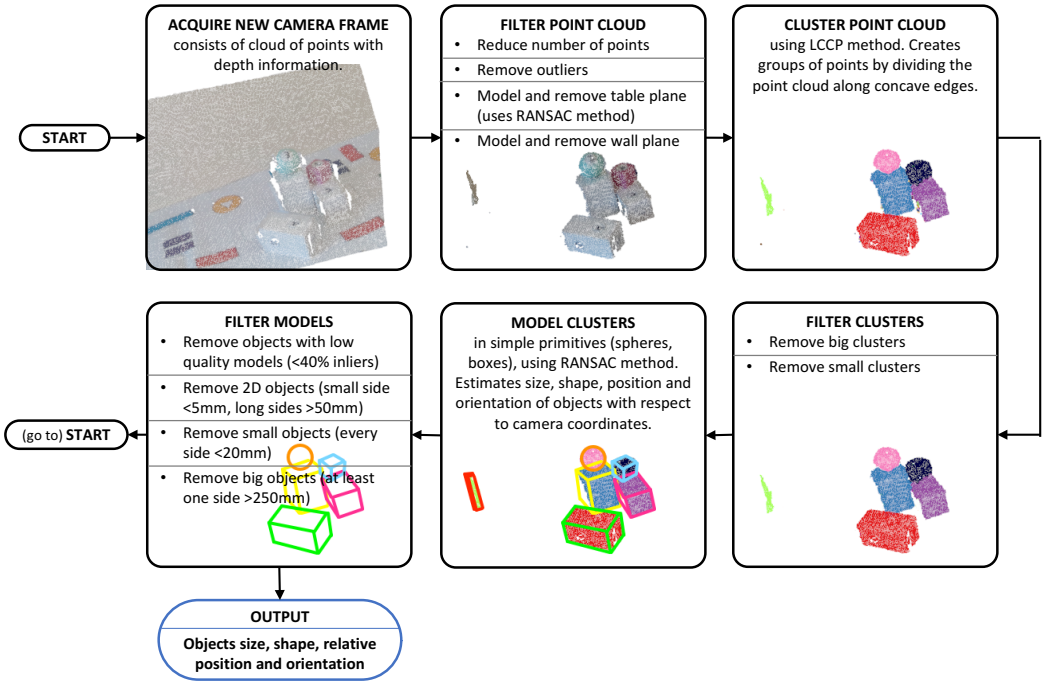

Appendix Figure 2 | Artificial Exteroception Module algorithm. The algorithm for artificial exteroception models the objects present on a flat surface (e.g., table). It is composed of six steps illustrated in the figure.

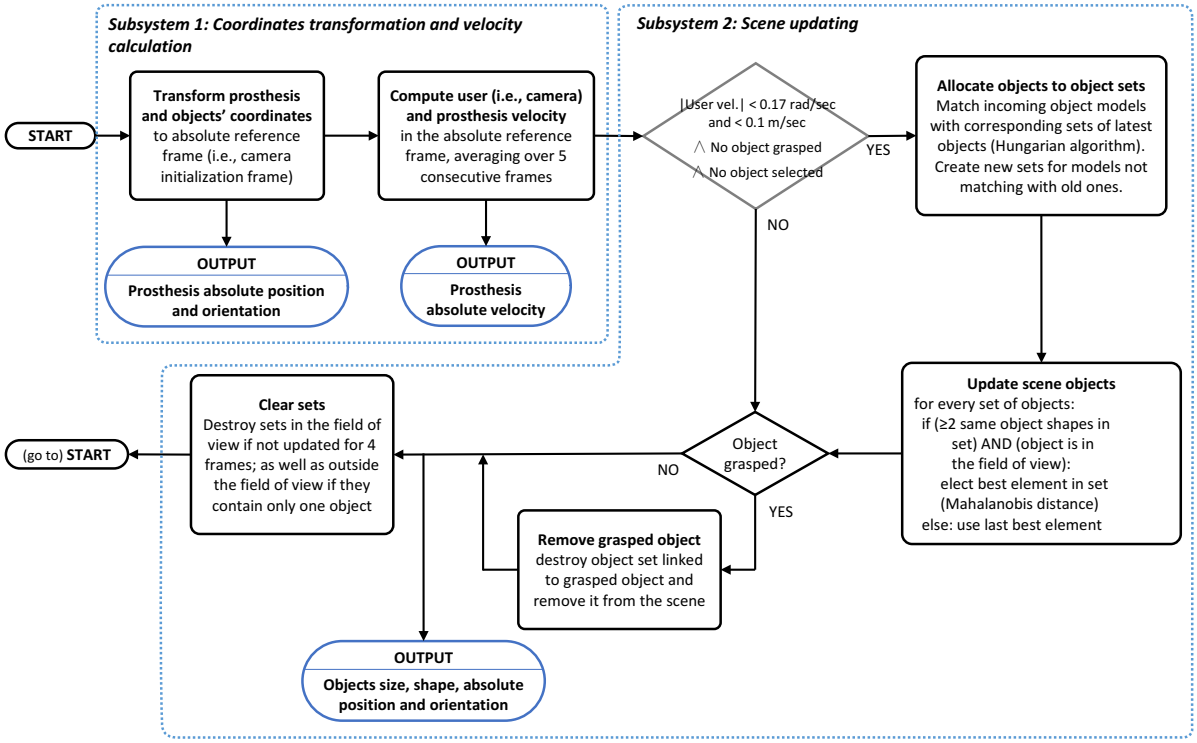

Appendix Figure 3 | Scene Generating Module algorithm. The algorithm for generating the scene consists of two subsystems. The first one transforms the coordinates of the objects and of the prosthesis to the absolute reference frame. It also computes the velocity of the camera and of the prosthesis. The velocity of the camera is used, together with the information received from the Preshape Control Module about grasped or selected objects, to decide whether to update the models of the objects in the scene. If the object models have to be updated, the newly modelled objects are matched with the ones in the scene based on their absolute position,

orientation, size and shape. Each object in the scene is member of a set containing the latest ten models matched with that object. The best member of each set is selected based on the Mahalanobis distance criteria, which accounts for the size, position, shape, and quality of the model. If an object is grasped, it is removed from the scene and the corresponding set of models is cleared. Lastly, it is possible that models are added to the scene but no real counterpart exists. These models are due to noise in the elaboration of the of the depth image or incorrect matching with the existing objects. This type of noise on the models is consistent over time. By removing objects that did not get any update for four consecutive frames, it is possible to obtain a scene which includes only models matching the real ones.

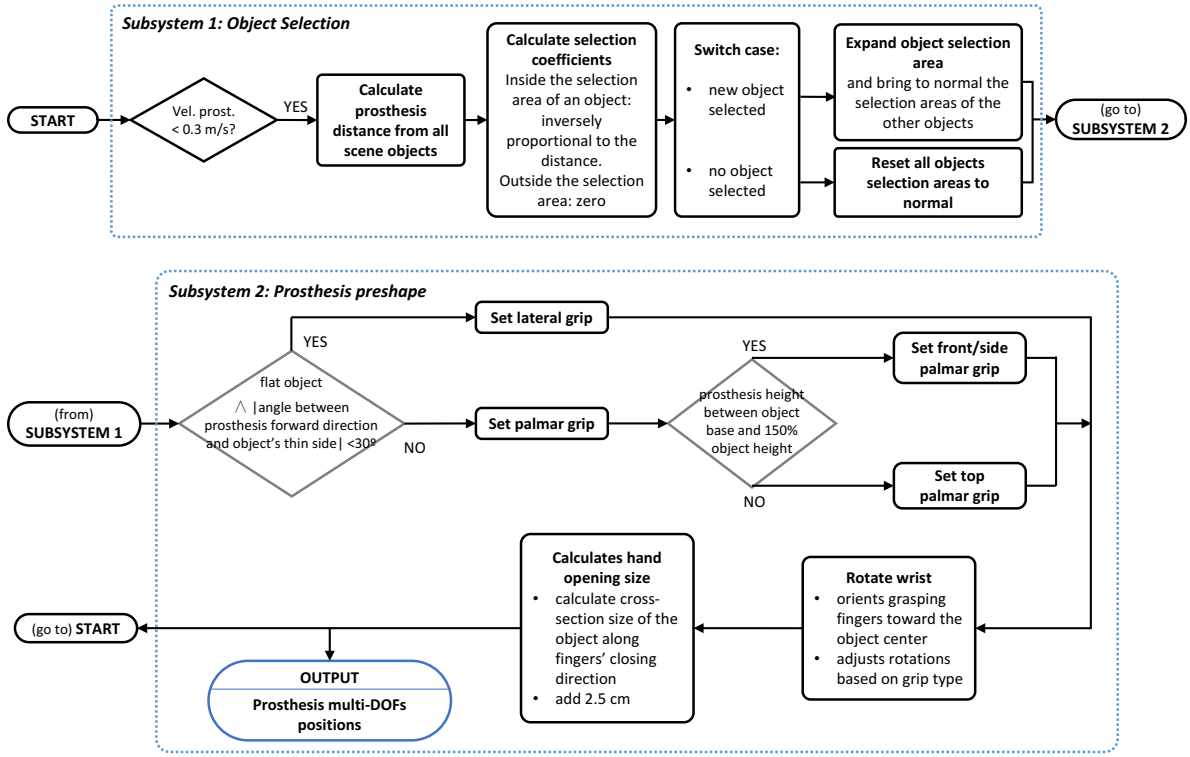

Appendix Figure 4 | Preshape Control Module algorithm. The preshape control module algorithm is responsible for selecting the object targeted by the user and preshaping the hand accordingly. Subsystem 1 handles the selection of the object. An object can be selected only if the prosthesis is moving slower than 0.3 m/s. This avoids selecting objects located in between the real target object and the prosthesis when the user is reaching them. Once an object is selected, its selection area is increased by 10%. This creates a buffer for keeping the current object selected even if the user moves slightly further away. This stabilizes the selection, especially in cluttered environments. Subsystem 2 handles the orientation of the prosthesis for the optimal grasp of the object. First of all, if an object is flat (e.g., a book, a CD-ROM) and the prosthesis is oriented toward its thin side, the lateral grip is selected to facilitate prehension. In all the other cases, palmar grip is selected. The DOFs of the wrist are adjusted so as to orient the grasping fingers (i.e., index, middle, thumb) toward the centre of the object. Small adjustments in wrist rotation and flexion are performed. Hand aperture is set 2.5 cm bigger than the width of the cross-section of the object along the direction in which the fingers close.

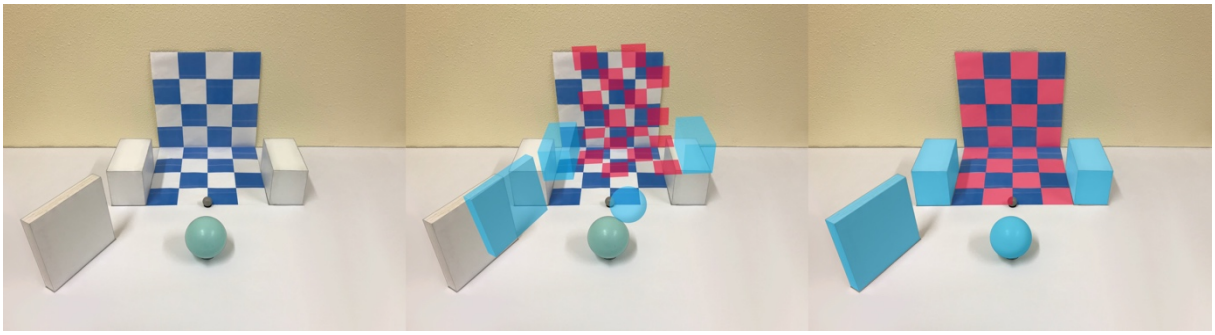

Appendix Figure 5 | Glasses calibration setups, with calibrated and uncalibrated AR feedback displayed. When the AR glasses are calibrated, the subject is presented with the glasses calibration setup (left figure). The retroreflective marker located at the base of the checkerboard allows for localization of the calibration setup with respect to the user. A virtual model of the setup is shown in the AR glasses (middle figure). The user is asked a series of questions regarding the projection he/she sees and the experimenter adjusts the glasses parameters (i.e., eyes position, position of (middle of) image plane, orientation of image plane, and (horizontal) field of view) accordingly. The questions refer to the size, perspective, position, and orientation of the objects and of the checkerboard. The procedure takes approximately 3 minutes. Once the glasses are calibrated, the user sees the virtual images superimposed with the real objects.

Bibliography

[1] K. Ziegler-Graham, E. J. MacKenzie, P. L. Ephraim, T. G. Travison, and R. Brookmeyer, “Estimating the Prevalence of Limb Loss in the United States: 2005 to 2050,” *Arch. Phys. Med. Rehabil.*, vol. 89, no. 3, pp. 422–429, 2008.

[2] J. W. Jones, S. A. Gruber, J. H. Barker, and W. C. Breidenbach, “Successful Hand Transplantation — One-Year Follow-up,” *N. Engl. J. Med.*, vol. 343, no. 7, pp. 468–473, 2000.

[3] R. M. Elliott, S. M. Tintle, and L. S. Levin, “Upper extremity transplantation: Current concepts and challenges in an emerging field,” *Curr. Rev. Musculoskelet. Med.*, vol. 7, no. 1, pp. 83–88, 2014.

[4] A. Fougner, O. Stavdahl, P. J. Kyberd, Y. G. Losier, and P. A. Parker, “Control of upper limb prostheses: Terminology and proportional myoelectric control: a review,” *IEEE Trans. Neural Syst. Rehabil. Eng.*, vol. 20, no. 5, pp. 663–677, 2012.

[5] “Sensor Hand Speed, Otto Bock GmbH.” [Online]. Available: https://media.ottobock.com/_web-site/prosthetics/upper-limb/myoelectric_devices/files/prosthesis_systems_information_for_practitioners.pdf. [Accessed: 27-Jan-2018].

[6] “Michelangelo Hand, Otto Bock GmbH.” [Online]. Available: https://www.ottobockus.com/media/local-media/prosthetics/upper-limb/michelangelo/files/michelangelo-brochure.pdf. [Accessed: 15-Jan-2018].

[7] M. Atzori and H. Muller, “Control Capabilities of Myoelectric Robotic Prostheses by Hand Amputees: A Scientific Research and Market Overview,” *Front Syst Neurosci*, vol. 9, no. November, p. 162, 2015.

[8] T. Feix, J. Romero, H. B. Schmiedmayer, A. M. Dollar, and D. Kragic, “The GRASP Taxonomy of Human Grasp Types,” *IEEE Trans. Human-Machine Syst.*, vol. 46, no. 1, 2016.

[9] “i-Limb Ultra, Touch Bionics Inc.” [Online]. Available: http://touchbionics.com/products/active-prostheses/i-limb-ultra. [Accessed: 15-Jan-2018].

[10] “DARPA.” [Online]. Available: https://www.darpa.mil/program/revolutionizing-prosthetics. [Accessed: 15-Jan-2018].

[11] E. A. Biddiss and T. T. Chau, “Upper limb prosthesis use and abandonment: a survey of the last 25 years.,” *Prosthet. Orthot. Int.*, vol. 31, no. 3, pp. 236–257, 2007.

[12] F. Cordella *et al.*, “Literature review on needs of upper limb prosthesis users,” *Front. Neurosci.*, vol. 10, no. MAY, pp. 1–14, 2016.

[13] T. R. D. Scott and M. Haugland, “Command and control interfaces for advanced neuroprosthetic applications,” in *Neuromodulation*, 2001, vol. 4, no. 4, pp. 165–174.

[14] D. Farina and S. Amsüss, “Reflections On The Present And Future Of Upper Limb Prostheses,” *Expert Rev. Med. Devices*, vol. 4440, no. May, p. 17434440.2016.1159511, Apr. 2016.

[15] N. Jiang, S. Dosen, K. R. Muller, and D. Farina, “Myoelectric Control of Artificial Limbs: Is There a Need to Change Focus? [In the Spotlight],” *IEEE Signal Process. Mag.*, vol. 29, no. 5, pp. 150–152, 2012.

[16] J. Gonzalez-Vargas, S. Dosen, S. Amsuess, W. Yu, and D. Farina, “Human-machine interface for the control of multi-function systems based on electrocutaneous menu: Application to multi-grasp prosthetic hands,” *PLoS One*, vol. 10, no. 6, pp. 1–26, 2015.

[17] A. E. Schultz and T. A. Kuiken, “Neural Interfaces for Control of Upper Limb Prostheses: The State of the Art and Future Possibilities,” *PM R*, vol. 3, no. 1, pp. 55–67, Jan. 2011.

[18] A. D. Roche, H. Rehbaum, D. Farina, and O. C. Aszmann, “Prosthetic Myoelectric Control Strategies: A Clinical Perspective,” *Curr. Surg. Reports*, vol. 2, no. 3, pp. 1–11, 2014.

[19] G. Schalk and E. C. Leuthardt, “Brain-computer interfaces using electrocorticographic signals,” *IEEE Rev. Biomed. Eng.*, vol. 4, pp. 140–154, 2011.

[20] J. S. Schofield, K. R. Evans, J. P. Carey, and J. S. Hebert, “Applications of sensory feedback in motorized upper extremity prosthesis: a review.,” *Expert Rev. Med. Devices*, vol. 13, no. May 2016, pp. 1–13, 2014.

[21] P. Svensson, U. Wijk, A. Björkman, and C. Antfolk, “A review of invasive and non-invasive sensory feedback in upper limb prostheses,” *Expert Rev. Med. Devices*, vol. 14, no. 6, pp. 439–447, Jun. 2017.

[22] B. T. Nghiem *et al.*, “Providing a Sense of Touch to Prosthetic Hands,” *Plast. Reconstr. Surg.*, vol. 135, no. 6, pp. 1652–1663, 2015.

[23] S. Micera, J. Carpaneto, and S. Raspopovic, “Control of hand prostheses using peripheral

information," *IEEE Rev. Biomed. Eng.*, vol. 3, no. January, pp. 48–68, 2010.
[24] B. Peerdeman *et al.*, "Myoelectric forearm prostheses: State of the art from a user-centered perspective," *J. Rehabil. Res. Dev.*, vol. 48, no. 6, p. 719, 2011.
[25] S. Amsuess, P. Goebel, B. Graimann, and D. Farina, "Extending mode switching to multiple degrees of freedom in hand prosthesis control is not efficient," *Conf. Proc. ... Annu. Int. Conf. IEEE Eng. Med. Biol. Soc. IEEE Eng. Med. Biol. Soc. Annu. Conf.*, vol. 2014, pp. 658–661, 2014.
[26] R. J. Bootsma and P. C. W. van Wieringen, "Spatio-temporal organisation of natural prehension," *Hum. Mov. Sci.*, vol. 11, no. 1–2, pp. 205–215, 1992.
[27] M. Markovic, S. Dosen, D. Popovic, B. Graimann, and D. Farina, "Sensor fusion and computer vision for context-aware control of a multi degree-of-freedom prosthesis.," *J. Neural Eng.*, vol. 12, no. 6, p. 66022, 2015.
[28] R. Tomović and G. Boni, "An Adaptive Artificial Hand," *IRE Trans. Autom. Control*, vol. AC-7, no. 3, pp. 3–10, 1962.
[29] R. Tomovic, G. Bekey, W. K.-R. and Automation, and U. 1987, "A strategy for grasp synthesis with multifingered robot hands," *Proc. IEEE Int. Conf. Robot. Autom.*, vol. 4, pp. 83–89, 1987.
[30] P. Chappell, J. Nightingale, … P. K.-J. of biomedical, and U. 1987, "Control of a single degree of freedom artificial hand," *J. Biomed. Eng.*, vol. 9, pp. 273–7, 1987.
[31] E. Banziger, "Wrist rotation activation in myoelectric prosthetics—an innovative approach: a case study," *ACPOC News*, 1996. [Online]. Available: http://www.acpoc.org/index.php/membership/newsletters-journals/acpoc-news-volumes-1995-2008/volume-2/number-4/wrist-rotation-activation-in-myoelectric-prosthetics----an-innovative-approach-a-case-study. [Accessed: 15-Jan-2018].
[32] E. D. Engeberg and S. G. Meek, "Adaptive sliding mode control for prosthetic hands to simultaneously prevent slip and minimize deformation of grasped objects," *IEEE/ASME Trans. Mechatronics*, vol. 18, no. 1, pp. 376–385, 2013.
[33] N. Wettels *et al.*, "Grip Control Using Biomimetic Tactile Sensing Systems," *IEEE/ASME Trans. Mechatronics*, vol. 14, pp. 718–23, 2009.
[34] D. Novak and R. Riener, "A survey of sensor fusion methods in wearable robotics," *Rob. Auton. Syst.*, vol. 73, pp. 155–170, 2014.
[35] C. M. Light, P. H. Chappell, B. Hudgins, and K. Engelhart, "Intelligent multifunction myoelectric control of hand prosthesis," *J. Med. Eng. Technol.*, vol. 26, no. 4, pp. 139–146, 2002.
[36] C. Cipriani, F. Zaccone, S. Micera, and M. C. Carrozza, "On the shared control of an EMG-controlled prosthetic hand: Analysis of user-prosthesis interaction," *IEEE Trans. Robot.*, vol. 24, no. 1, pp. 170–184, 2008.
[37] G. Ghazaei, A. Alameer, P. Degenaar, G. Morgan, and K. Nazarpour, "Deep learning-based artificial vision for grasp classification in myoelectric hands," *J. Neural Eng.*, vol. 14, no. 3, 2017.
[38] J. Degol, A. Akhtar, B. Manja, and T. Bretl, "Automatic grasp selection using a camera in a hand prosthesis," *Proc. Annu. Int. Conf. IEEE Eng. Med. Biol. Soc. EMBS*, vol. 2016–Octob, pp. 431–434, 2016.
[39] D. P. McMullen *et al.*, "Demonstration of a semi-autonomous hybrid brain-machine interface using human intracranial EEG, eye tracking, and computer vision to control a robotic upper limb prosthetic," vol. 22, no. 4, pp. 784–796, 2014.
[40] M. Markovic, S. Dosen, C. Cipriani, D. Popovic, and D. Farina, "Stereovision and augmented reality for closed-loop control of grasping in hand prostheses.," *J. Neural Eng.*, vol. 11, no. 4, p. 46001, 2014.
[41] D. Novak and R. Riener, "Enhancing patient freedom in rehabilitation robotics using gaze-based intention detection," *IEEE Int. Conf. Rehabil. Robot.*, 2013.
[42] "COAPT." [Online]. Available: http://coaptengineering.com/. [Accessed: 27-Jan-2018].
[43] E. Scheme and K. Englehart, "Electromyogram pattern recognition for control of powered upper-limb prostheses: State of the art and challenges for clinical use," *J. Rehabil. Res. Dev.*, vol. 48, no. 6, pp. 643–660, 2011.
[44] R. Liu, Y. X. Wang, and L. Zhang, "An FDES-Based shared control method for asynchronous brain-actuated robot," *IEEE Trans. Cybern.*, vol. 46, no. 6, pp. 1452–1462, 2016.
[45] L. Tonin, R. Leeb, M. Tavella, S. Perdikis, J. R. Del Millán, and J. del R. Millan, "The role of shared-control in BCI-based telepresence," *Conf. Proc. - IEEE Int. Conf. Syst. Man Cybern.*, pp. 1462–1466, 2010.
[46] J. Philips *et al.*, "Adaptive shared control of a brain-actuated simulated wheelchair," *2007 IEEE 10th Int. Conf. Rehabil. Robot. ICORR'07*, vol. 0, no. c, pp. 408–414, 2007.
[47] F. Galán *et al.*, "A brain-actuated wheelchair: Asynchronous and non-invasive Brain-computer interfaces for continuous control of robots," *Clin. Neurophysiol.*, vol. 119, no. 9, pp. 2159–2169,

2008.
[48] A. R. Satti, D. Coyle, and G. Prasad, “Self-paced brain-controlled wheelchair methodology with shared and automated assistive control,” *IEEE SSCI 2011 - Symp. Ser. Comput. Intell. - CCMB 2011 2011 IEEE Symp. Comput. Intell. Cogn. Algorithms, Mind, Brain*, pp. 120–127, 2011.
[49] T. Carlson and Y. Demiris, “Collaborative control for a robotic wheelchair: Evaluation of performance, attention, and workload,” *IEEE Trans. Syst. Man, Cybern. Part B Cybern.*, vol. 42, no. 3, pp. 876–888, 2012.
[50] D. A. Bennett and M. Goldfarb, “IMU-Based Wrist Rotation Control of a Transradial Myoelectric Prosthesis,” *IEEE Trans. Neural Syst. Rehabil. Eng.*, vol. 4320, no. c, pp. 1–1, 2017.
[51] S. Dosen, M. Markovic, C. Hartmann, and S. Member, “Sensory Feedback in Prosthetics : A Standardized Test Bench for Closed-Loop Control,” vol. 23, no. 2, pp. 267–276, 2015.
[52] S. C. Stein, F. Wörgötter, M. Schoeler, J. Papon, and T. Kulvicius, “Convexity based object partitioning for robot applications,” *Proc. - IEEE Int. Conf. Robot. Autom.*, pp. 3213–3220, 2014.
[53] M. a Fischler and R. C. Bolles, “Random Sample Consensus: A Paradigm for Model Fitting with Applications to Image Analysis and Automated Cartography,” *Commun. ACM*, vol. 24, no. 6, pp. 381–395, 1981.
[54] J. Aulinas, Y. Petillot, J. Salvi, and X. Lladó, “The SLAM problem: A survey,” *Front. Artif. Intell. Appl.*, vol. 184, no. 1, pp. 363–371, 2008.
[55] D. Bruff, “The Assignment Problem and the Hungarian Method.” 2005.
[56] R. De Maesschalck, D. Jouan-Rimbaud, and D. L. L. Massart, “The Mahalanobis distance,” *Chemom. Intell. Lab. Syst.*, vol. 50, no. 1, pp. 1–18, 2000.
[57] J. Fan, J. He, and S. I. H. Tillery, “Control of hand orientation and arm movement during reach and grasp,” *Exp. Brain Res.*, vol. 171, no. 3, pp. 283–296, 2006.
[58] A. Fougner, E. Scheme, A. D. C. Chan, K. Englehart, and Ø. Stavdahl, “Resolving the limb position effect in myoelectric pattern recognition,” *IEEE Trans. Neural Syst. Rehabil. Eng.*, vol. 19, no. 6, pp. 644–651, 2011.
[59] NASA, “Nasa Task Load Index (TLX),” vol. v 1.0 Manu, 1986.
[60] M. Štrbac, S. Kočović, M. Marković, and D. B. Popović, “Microsoft Kinect based artificial perception system for control of functional electrical stimulation assisted grasping,” vol. 2014, pp. 1–13, 2014.
[61] S. Amsuess, P. Goebel, B. Graimann, and D. Farina, “A multi-class proportional myocontrol algorithm for upper limb prosthesis control: Validation in real-life scenarios on amputees,” *IEEE Trans. Neural Syst. Rehabil. Eng.*, vol. 23, no. 5, 2015.
[62] W. Hill, Ø. Stavdahl, L. N. Hermansson, P. Kyberd, S. Swanson, and S. Hubbard, “Functional Outcomes in the WHO-ICF Model: Establishment of the Upper Limb Prosthetic Outcome Measures Group,” *JPO J. Prosthetics Orthot.*, vol. 21, no. 2, pp. 115–119, Apr. 2009.
[63] W. Hill *et al.*, “Upper Limb Prosthetic Outcome Measures (ULPOM): A Working Group and Their Findings,” *J. Prosthetics Orthot.*, no. 21, pp. P69-82, 2009.
[64] H. Y. N. Lindner, B. S. Nätterlund, and L. M. N. Hermansson, “Upper limb prosthetic outcome measures: review and content comparison based on International Classification of Functioning, Disability and Health.,” *Prosthet. Orthot. Int.*, vol. 34, no. 2, pp. 109–28, 2010.